# HIGH FREQUENCY BEHAVIOR OF THE FOCUSING NONLINEAR SCHRÖDINGER EQUATION WITH RANDOM INHOMOGENEITIES

ALBERT FANNJIANG *, SHI JIN †, AND GEORGE PAPANICOLAOU ‡

**Abstract.** We consider the effect of random inhomogeneities on the focusing singularity of the nonlinear Schrödinger equation in three dimensions, in the high frequency limit. After giving a phase space formulation of the high frequency limit using the Wigner distribution, we derive a nonlinear diffusion equation for the evolution of the wave energy density when random inhomogeneities are present. We show that this equation is linearly stable even in the case of a focusing nonlinearity provided that it is not too strong. The linear stability condition is related to the variance identity for the nonlinear Schrödinger equation in an unexpected way. We carry out extensive numerical computations to get a better understanding of the interaction between the focusing nonlinearity and the randomness.

**1. Introduction.** The nonlinear Schrödinger equation (NLS)

$$
\begin{aligned}
& i\frac{\partial\phi}{\partial t} + \frac{1}{2}\Delta\phi - \beta|\phi|^2\phi = 0 \\
& \phi(0, \mathbf{x}\,) = \phi_0(\mathbf{x}),
\end{aligned} \tag{1}
$$

with $\mathbf{x}$ in three dimensions, arises as the subsonic limit of the Zakharov model of Langmuir equations in plasma physics [19] and in many other contexts. The NLS equation (1) is in dimensionless form with $\beta$ a parameter that measures the strength of the nonlinearity relative to wave dispersion. When $\beta < 0$ the nonlinearity is focusing and when $\beta > 0$ it is defocusing. An important property of NLS is that, in three dimensions, the solution in the focusing case may develop a singularity at some finite time. This result is based on the existence of two invariants with respect to time: the **mass**

$$
M = \int_{R^3} |\phi(t,\mathbf{x})|^2 d\mathbf{x} \tag{2}
$$

and the **energy**

$$
H = \int_{R^3} \left( \frac{1}{2}|\nabla\phi(t,\mathbf{x})|^2 + \frac{1}{2}\beta|\phi(t,\mathbf{x})|^4 \right) d\mathbf{x}, \tag{3}
$$

together with the **variance identity**

$$
\frac{d^2}{dt^2}\int_{R^3} |\mathbf{x}|^2|\phi(t,\mathbf{x})|^2\, d\mathbf{x} = 8H + 2\beta\int_{R^3} |\phi(t,\mathbf{x})|^4\, d\mathbf{x}\ . \tag{4}
$$

In the focusing case $\beta < 0$ and with a negative energy $H < 0$, the solution cannot remain bounded for all time. More precisely, it follows from the variance identity and the uncertainty inequality that the $L^2$ norm of the gradient of the solution blows up in finite time [6]. Many other properties of NLS can be found in [17].

---

*Department of Mathematics, University of California, Davis, CA, 95616. Research supported by NSF grants DMS-9600119, DMS-9707756 and DMS-9971322

†School of Mathematics, Georgia Institute of Technology, Atlanta, GA 30332. Research supported by AFOSR grant F49620-92-J0098, NSF grants DMS-9404157 and DMS-9704957.

‡Department of Mathematics, Stanford University, Stanford, CA 94305. Research supported by by AFOSR grant F49620-98-1-0211 and by NSF grants DMS-9622854

The goal of this paper is to investigate the effect of random inhomogeneities on the focusing NLS in the **high frequency** regime. In the absence of the regularizing effect of the random inhomogeneities the initial value problem for the focusing NLS is, in this regime, catastrophically ill-posed, even if the original NLS does not blow up. The random inhomogeneities are modeled by a potential that is a zero mean, stationary random function with correlation length comparable to the wavelength, and with small variance. Using the Wigner phase space form of the Schrödinger equation we derive a nonlinear mean field transport approximation, in the high frequency and weak fluctuation limit. When, moreover, the transport mean free path is small, this nonlinear, phase space transport equation can be further approximated by a nonlinear degenerate diffusion equation (equation (73)). This is the main result of this paper, and it captures in a precise way the interaction between the focusing nonlinearity and the random medium, in the high frequency limit. A linear stability analysis of this diffusion equation reveals in a simplified but physically clear way the form of the nonlinearity-randomness interaction. We find that the condition that the linearized diffusion equation be stable reduces to the **positivity of the right hand of the variance identity (4) of NLS**, in the high frequency limit (equation (91)). This is a surprising result because it is precisely the opposite of this condition, a negative right hand side for (4), which produces a focusing singularity in NLS (1). We see that this condition, or rather its opposite

$$8H + 2\beta \int_{R^3} |\phi(t,\mathbf{x})|^4 \, d\mathbf{x} > 0 \tag{5}$$

becomes a **stability** condition, in a well defined high frequency regime, provided that the focusing mechanism is regularized by random inhomogeneities.

The paper is organized as follows. In section 2 we review briefly the nonlinear high frequency limit in its usual form and in section 3 we reconsider it in its phase space form, using the Wigner distribution. In section 4 the random initial data is discussed. In section 5 we introduce random inhomogeneities and describe the mean field, transport approximation for the Wigner distribution. In section 6 we rewrite the nonlinear transport equation in parity form, introducing the odd and even parts of the Wigner distribution, and in section 7 we derive the diffusion approximation, in the small mean free path limit. The linearized stability condition for this degenerate, nonlinear diffusion equation is obtained in section 8.

In section 9 we introduce a numerical scheme for the mean field, nonlinear transport equation and present the results of several numerical calculations. In section 10 we do the same for the degenerate nonlinear diffusion equation for the wave energy density. Our numerical results indicate that in the high frequency regime the random inhomogeneities slow down the propagation of wave energy, in the linear and defocusing cases. In the focusing case, the randomness is able to interact fully with the focusing nonlinearity as long as the nonlinearity is not too strong. In the diffusive regime, the randomness interacts fully with the focusing or defocusing nonlinearity, in a diffusive way, provided that the stability condition (91) holds. We end with section 11 that contains a brief summary and conclusions.

**2. Nonlinear high frequency limit.** We review briefly the high frequency asymptotic analysis for solutions of (1) with oscillatory initial data. In the high frequency limit the dimensionless time and propagation distance are long compared to the scale of variation of the potential $V(\mathbf{x})$. To make this precise we introduce slow time and space variables $t \to t/\epsilon$, $\mathbf{x} \to \mathbf{x}/\epsilon$, with $\epsilon$ a small parameter, and the scaled wave function $\phi^\epsilon(t,\mathbf{x}) = \phi(t/\epsilon, \mathbf{x}/\epsilon)$, which satisfies the scaled Schrödinger equation

$$
\begin{aligned}
&i\epsilon\phi_t^\epsilon + \frac{\epsilon^2}{2}\Delta\phi^\epsilon - V(t,\mathbf{x})\phi^\epsilon = 0, \\
&V(t,\mathbf{x}) = \beta|\phi(t,\mathbf{x})|^2 + V_0(\mathbf{x}).
\end{aligned} \tag{6}
$$

The potential has the nonlinear part from the NLS and a linear part that we may add since it does not affect the analysis as long as it does not depend on $\epsilon$. In the usual high frequency approximation [11] we consider initial data of the form

$$
\phi^\epsilon(0,\mathbf{x}) = e^{iS_0(\mathbf{x})/\epsilon}A_0(\mathbf{x}) \tag{7}
$$

with a smooth, real valued initial phase function $S_0(\mathbf{x})$ and a smooth compactly supported complex valued initial amplitude $A_0(\mathbf{x})$. We then look for an asymptotic solution of (6) in the same form as the initial data (7), with evolved phase and amplitude

$$
\phi^\epsilon(t,\mathbf{x}) \sim e^{iS(t,\mathbf{x})/\epsilon}A(t,\mathbf{x}). \tag{8}
$$

Inserting this form into (6) and equating powers of $\epsilon$ we get approximate evolution equations for the phase and amplitude

$$
S_t + \frac{1}{2}|\nabla S|^2 + V(t,\mathbf{x}) = 0, \qquad S(0,\mathbf{x}) = S_0(\mathbf{x}) \tag{9}
$$

and

$$
(|A|^2)_t + \nabla\cdot(|A|^2\nabla S) = 0, \qquad |A(0,\mathbf{x})|^2 = |A_0(\mathbf{x})|^2. \tag{10}
$$

The phase equation (9) is the *eiconal* and the amplitude equation (10) the *transport* equation. The terminology for the latter is standard in the high frequency approximation but should not be confused with the radiative transport equation that will be derived later. These equations can be rewritten using the high frequency dispersion relation, $\omega$, of the Schrödinger equation

$$
\omega(t,\mathbf{x},\mathbf{k}) = \frac{1}{2}|\mathbf{k}|^2 + V(t,\mathbf{x}). \tag{11}
$$

The energy in the high frequency regime is obtained by using the ansatz (8) in the energy (3) so that for small $\epsilon$

$$
H \approx \int_{R^3} (\frac{1}{2}|\nabla S|^2 + \frac{\beta}{2}|A|^2 + V_0)|A|^2 d\mathbf{x}. \tag{12}
$$

The potential is $V(t,\mathbf{x}) = \beta|A(t,\mathbf{x})|^2 + V_0(\mathbf{x})$. Even when it does not depend on the amplitude $|A|$, in the linear case, the eiconal equation (9) is nonlinear and its solution exists in general only up to some time $t^*$ that depends on the initial phase $S_0(\mathbf{x})$ and $V_0(\mathbf{x})$. This solution can be constructed by the method of characteristics and singularities form when these characteristics (rays) cross. The eiconal and the transport equations are decoupled in the linear case.

To see more clearly the form of the eiconal and transport equations in the NLS case, we let $\rho = |A|^2, \mathbf{u} = \nabla S$, take the gradient of (9), with only the nonlinear potential $V(t,\mathbf{x}) = \beta|A(t,\mathbf{x})|^2$, and rewrite this differentiated eiconal and (10) in conservation law form:

$$\rho_t + \nabla \cdot (\rho\mathbf{u}) = 0, \tag{13}$$

$$(\rho\mathbf{u})_t + \nabla \cdot (\rho\mathbf{u}\mathbf{u}) + \nabla p(\rho) = 0, \tag{14}$$

where

$$p(\rho) = \frac{\beta}{2}\rho^2. \tag{15}$$

Now the eiconal and transport equations are fully coupled. When $\beta > 0$, this system of conservation laws are the isentropic gas dynamics equations, with equation of state given by (15) ($\gamma$-law gas with $\gamma = 2$). It is hyperbolic, and the solution may become discontinuous at a finite time. The velocity $\mathbf{u}$ is irrotational since it is a gradient, so $\nabla \times \mathbf{u} = 0$. The eiconal equation (9) is the Bernoulli form of the momentum conservation law (14) for time dependent and irrotational flows. Another form of the momentum conservation law is

$$\rho(\mathbf{u}_t + \mathbf{u} \cdot \nabla\mathbf{u}) + \nabla p = 0 \tag{16}$$

and the conservation of energy is exactly as in (12) with $V_0 = 0$, which we rewrite in the fluid variables

$$\frac{\partial}{\partial t}H = \frac{\partial}{\partial t}\int_{R^3}(\frac{1}{2}\rho|\mathbf{u}|^2 + p)d\mathbf{x} = 0 \tag{17}$$

In the one-dimensional defocusing case, the nonlinear high frequency limit was analyzed in detail in [9, 10]. In the higher dimensional defocusing case, mathematical results are only available for the more regular Schrödinger-Poisson high frequency equations [5, 13, 7]. When $\beta < 0$, the system of conservation laws (13)-(14) has complex characteristics and the initial value problem is catastrophically ill-posed. This is the case even if the original NLS does not have solutions that blow up, when the Hamiltonian $H > 0$, for example. Thus the high frequency limit for the focusing NLS, without any regularizing mechanisms, does not make sense physically or mathematically.

**3. The Wigner distribution.** An essential step in deriving phase space transport equations from wave equations is the introduction of the Wigner distribution [18, 14]. We begin with a brief review of some basic facts and then give the phase space form of the high frequency limit.

For any smooth function $\phi$, rapidly decaying at infinity, the Wigner distribution is defined by

$$W(\mathbf{x},\mathbf{k}) = \left(\frac{1}{2\pi}\right)^3 \int_{R^3} e^{i\mathbf{k}\cdot\mathbf{y}}\phi(\mathbf{x} - \frac{\mathbf{y}}{2})\overline{\phi}(\mathbf{x} + \frac{\mathbf{y}}{2})d\mathbf{y} \tag{18}$$

where $\bar{\phi}$ is the complex conjugate of $\phi$. The Wigner distribution is defined on phase space and has many important properties. It is real and its $\mathbf{k}$-integral is the modulus square of the function $\phi$,

$$\int_{R^3} W(\mathbf{x},\mathbf{k})d\mathbf{k} = |\phi(\mathbf{x})|^2, \tag{19}$$

so we may think of $W(\mathbf{x},\mathbf{k})$ as wave number-resolved mass density. This is not quite right though because $W(\mathbf{x},\mathbf{k})$ is not always positive but it does become positive in the high frequency limit. The energy flux is expressed through $W(\mathbf{x},\mathbf{k})$ by

$$\mathcal{F} = \frac{1}{2i}(\phi\nabla\overline{\phi} - \overline{\phi}\nabla\phi) = \int_{R^3} \mathbf{k}W(\mathbf{x},\mathbf{k})d\mathbf{k} \tag{20}$$

and its second moment in $\mathbf{k}$ is

$$\int |\mathbf{k}|^2 W(\mathbf{x},\mathbf{k})d\mathbf{k} = |\nabla\phi(\mathbf{x})|^2. \tag{21}$$

The Wigner distribution possesses an important $\mathbf{x}$-to-$\mathbf{k}$ duality given by the alternative definition

$$W(\mathbf{x},\mathbf{k}) = \int e^{i\mathbf{p}\cdot\mathbf{x}}\hat{\phi}(-\mathbf{k}-\frac{\mathbf{p}}{2})\overline{\hat{\phi}(-\mathbf{k}+\frac{\mathbf{p}}{2})}d\mathbf{p}. \tag{22}$$

where $\hat{\phi}$ is the Fourier transform of $\phi$

$$\hat{\phi}(\mathbf{k}) = \frac{1}{(2\pi)^3}\int e^{i\mathbf{k}\cdot\mathbf{x}}\phi(\mathbf{x})d\mathbf{x}. \tag{23}$$

These properties make the Wigner distribution a good quantity for analyzing the evolution of wave energy in phase space.

Given a wave function of the form (8), that is, an inhomogeneous wave with phase $S(t,\mathbf{x})/\epsilon$, its scaled Wigner distribution has the weak limit

$$W^\epsilon(\mathbf{x},\mathbf{k}) = \frac{1}{\epsilon^3}W(\mathbf{x},\frac{\mathbf{k}}{\epsilon}) \to |A(\mathbf{x})|^2\delta(\mathbf{k}-\nabla S(\mathbf{x})), \tag{24}$$

as a generalized function, as $\epsilon \to 0$. This suggests that the correct scaling for the high frequency limit is

$$W^\epsilon(t,\mathbf{x},\mathbf{k}) = \left(\frac{1}{2\pi}\right)^3 \int e^{i\mathbf{k}\cdot\mathbf{y}}\phi^\epsilon(t,\mathbf{x}-\frac{\epsilon\mathbf{y}}{2})\overline{\phi^\epsilon(t,\mathbf{x}+\frac{\epsilon\mathbf{y}}{2})}d\mathbf{y}\,, \tag{25}$$

where $\phi^\epsilon$ satisfies (6). From (24) we conclude that as $\epsilon \to 0$ the scaled Wigner distribution of the solution $\phi^\epsilon(t,\mathbf{x})$ of (6) with initial data (7) is given by

$$W(t,\mathbf{x},\mathbf{k}) = |A(t,\mathbf{x})|^2\delta(\mathbf{k}-\nabla S(t,\mathbf{x})), \tag{26}$$

where $S(t,\mathbf{x})$ and $A(t,\mathbf{x})$ are solutions of the eiconal and transport equations (9) and (10), respectively.

We will now sketch the derivation of the high frequency approximation of the scaled Wigner distribution directly from the Schrödinger equation. Let us assume that the initial Wigner distribution $W_0^\epsilon(\mathbf{x},\mathbf{k})$ tends to a smooth function $W_0(\mathbf{x},\mathbf{k})$ that has compact support. Note that this is not the case with the Wigner function corresponding to $\phi^\epsilon(0,\mathbf{x})$ given by (7) but it may be the case for random initial wave functions. We explain this briefly in the next section. The evolution equation for $W^\epsilon(t,\mathbf{x},\mathbf{k})$ corresponding to the Schrödinger equation (6) is the **Wigner equation**

$$W_t^\epsilon + \mathbf{k}\cdot\nabla_{\mathbf{x}}W^\epsilon + \mathcal{L}^\epsilon W^\epsilon = 0. \tag{27}$$

Here the operator $\mathcal{L}^\epsilon$ is defined by

$$\mathcal{L}^\epsilon Z(\mathbf{x},\mathbf{k}) = i\int_{R^3} e^{-i\mathbf{p}\cdot\mathbf{x}}\hat{V}(\mathbf{p})\frac{1}{\epsilon}\left[Z(\mathbf{x},\mathbf{k}+\frac{\epsilon\mathbf{p}}{2}) - Z(\mathbf{x},\mathbf{k}-\frac{\epsilon\mathbf{p}}{2})\right] d\mathbf{p} \tag{28}$$

on any smooth function $Z$ in phase space. The Fourier transform of $V$ is $\hat{V}$.

From (28) we can find easily the limit of the operator $\mathcal{L}^\epsilon$ as $\epsilon \to 0$, in the linear case where the potential $V$ does not depend on the solution. For any smooth and decaying function $Z(\mathbf{x},\mathbf{k})$ we have

$$\mathcal{L}^\epsilon Z(\mathbf{x},\mathbf{k}) \to -\nabla_{\mathbf{x}}V\cdot\nabla_{\mathbf{k}}Z. \tag{29}$$

Thus, the limit Wigner equation is the **Liouville equation** in phase space

$$W_t + \mathbf{k}\cdot\nabla_{\mathbf{x}}W - \nabla V\cdot\nabla_{\mathbf{k}}W = 0 \tag{30}$$

with the initial condition $W(0,\mathbf{x},\mathbf{k}) = W_0(\mathbf{x},\mathbf{k})$. When the initial Wigner distribution has the form

$$W_0(\mathbf{x},\mathbf{k}) = |A_0(\mathbf{x})|^2\delta(\mathbf{k}-\nabla S_0(\mathbf{x})) \tag{31}$$

then it is easy to see that, up to the time of singularity formation, the solution of (30) is given by

$$W(t,\mathbf{x},\mathbf{k}) = |A(t,\mathbf{x})|^2\delta(\mathbf{k}-\nabla S(t,\mathbf{x})) \tag{32}$$

where $S(t,\mathbf{x})$ and $A(t,\mathbf{x})$ are solutions of the eiconal and transport equations (9) and (10), respectively. If the $W_0(\mathbf{x},\mathbf{k})$ and $V(\mathbf{x})$ are smooth so will be the solution of (29), in the linear case.

In the nonlinear case the potential depends on the solution. The Liouville, or **Liouville-Vlasov**, equation is a nonlinear partial differential equation since

$$V = \beta\rho(t,\mathbf{x}) + V_0(\mathbf{x}) \quad \text{and} \quad \rho = \int_{R^3} W d\mathbf{k}\,. \tag{33}$$

For the initial conditions (31) it is better to use the fluid variables

$$\rho(t,\mathbf{x}) = |A(t,\mathbf{x})|^2 \quad \text{and} \quad \rho(t,\mathbf{x})\mathbf{u}(t,\mathbf{x}) = \rho(t,\mathbf{x})\nabla S(t,\mathbf{x}) = \int_{R^3}\mathbf{k}W d\mathbf{k} \tag{34}$$

which solve the conservation laws (13)-(14). In the defocusing case, up to the time of shock formation the solution to the Liouville-Vlasov equation is given by

$$W(t,\mathbf{x},\mathbf{k}) = \rho(t,\mathbf{x})\delta(\mathbf{k}-\mathbf{u}(t,\mathbf{x})). \tag{35}$$

We see, therefore, that from the Wigner distribution we can recover all the information about the high frequency approximation, when it makes sense. In addition, it provides flexibility to deal with initial data that are not of the form (31).

**4. Random initial data.** Let us consider initial wave functions of the form $\phi_0(\frac{\mathbf{x}}{\epsilon},\mathbf{x})$ where $\phi_0(\mathbf{y},\mathbf{x})$is a stationary random field in $\mathbf{y}$ for each $\mathbf{x}$ with mean zero and covariance

$$\langle\phi_0(\mathbf{y}_1,\mathbf{x}_1)\bar{\phi}_0(\mathbf{y}_2,\mathbf{x}_2)\rangle = R_0(\mathbf{y}_1-\mathbf{y}_2,\mathbf{x}_1,\mathbf{x}_2). \tag{36}$$

Then with

$$W_0^\epsilon(\mathbf{x},\mathbf{k}) = \frac{1}{(2\pi)^3}\int e^{i\mathbf{k}\cdot\mathbf{y}}\phi_0(\frac{\mathbf{x}}{\epsilon}-\frac{\mathbf{y}}{2},\mathbf{x}-\frac{\epsilon\mathbf{y}}{2})\bar{\phi}_0(\frac{\mathbf{x}}{\epsilon}+\frac{\mathbf{y}}{2},\mathbf{x}+\frac{\epsilon\mathbf{y}}{2})d\mathbf{y} \tag{37}$$

we have that

$$\langle W_0^\epsilon(\mathbf{x},\mathbf{k})\rangle \to \hat{R}_0(\mathbf{k},\mathbf{x},\mathbf{x}) \tag{38}$$

pointwise in $\mathbf{k}$ and $\mathbf{x}$. Here $\hat{R}_0(\mathbf{k},\mathbf{x},\mathbf{x})$ is the diagonal part of the power spectral density of $R_0$, that is, its Fourier transform in $\mathbf{y}$ with $\mathbf{x}_1 = \mathbf{x}_2 = \mathbf{x}$. We also have that for any test function $\psi(\mathbf{x},\mathbf{k})$

$$\int W_0^\epsilon(\mathbf{x},\mathbf{k})\psi(\mathbf{x},\mathbf{k})d\mathbf{x}d\mathbf{k} \to \int \hat{R}_0(\mathbf{k},\mathbf{x},\mathbf{x})\psi(\mathbf{x},\mathbf{k})d\mathbf{x}d\mathbf{k} \tag{39}$$

in probability as $\epsilon \to 0$. This means that $W_0^\epsilon$ converges to $\hat{R}_0$ weakly in probability. However, it does not converge in mean square, that is, the mean fluctuation $\langle ||W_0^\epsilon - \hat{R}_0||_{L^2}^2\rangle$ does not go to zero. This can be seen from the fact that $\langle ||W_0^\epsilon||_{L^2}^2\rangle$ does not tend to $||\hat{R}_0||_{L^2}^2$.

From the above example we see how smooth and compactly supported initial Wigner functions can arise. For linear waves in random media there are no additional complications when dealing with random initial data that are statistically independent from the medium. The situation is much more complicated in the case of nonlinear waves, and essentially unexplored mathematically.

**5. High frequency limit with random inhomogeneities .** We now consider small random perturbations of the potential $V(t,\mathbf{x})$. It is well known that in one space dimension, linear waves in a random medium get localized even when the random perturbations are small [15], so our analysis is restricted to three dimensions. The two dimensional case is difficult because the mean field approximation that we use in three dimensions is most likely incorrect.

We consider the linear case first. We assume that the correlation length of the random perturbation is of the same order as the wavelength, so the potential has the form $V(t,\mathbf{x}) + V_1(\frac{\mathbf{x}}{\epsilon})$ since the wavelength is of order $\epsilon$. Here $V(t,\mathbf{x})$ is the slowly varying background, without the nonlinear part, and $V_1(\mathbf{y})$ is a mean zero, stationary random function with correlation length of order one. This scaling allows the random potential to interact fully with the waves. We shall also assume that the fluctuations are statistically homogeneous and isotropic so that

$$\langle V_1(\mathbf{x})V_1(\mathbf{y})\rangle = R(|\mathbf{x}-\mathbf{y}|), \tag{40}$$

where $\langle,\rangle$ denotes statistical averaging and $R(|\mathbf{x}|)$ is the covariance of random fluctuations. The power spectrum of the fluctuations is defined by

$$\hat{R}(\mathbf{k}) = \left(\frac{1}{2\pi}\right)^3 \int e^{i\mathbf{k}\cdot\mathbf{x}}R(\mathbf{x})d\mathbf{x}. \tag{41}$$

When (40) holds, the fluctuations are isotropic and $\hat{R}$ is a function of $|\mathbf{k}|$ only. Because of the statistical homogeneity, the Fourier transform of the random potential $V_1$ is a generalized random process with orthogonal increments

$$\langle \hat{V}_1(\mathbf{p})\hat{V}_1(\mathbf{q})\rangle = \hat{R}(\mathbf{p})\delta(\mathbf{p}+\mathbf{q}). \tag{42}$$

If the amplitude of these fluctuations is strong then scattering will dominate and waves will be localized [4], at least in the linear case. This means that we cannot assume that the fluctuations in the random potential $V_1(\mathbf{y})$ are large. If the random fluctuations are too weak they will not affect energy transport at all. In order that the scattering produced by the random potential and the influence of the slowly varying background affect energy transport in comparable ways the fluctuations in the random potential must be of order $\sqrt{\epsilon}$. This makes the transport mean free time, the reciprocal of $\Sigma$ below, of order one and independent of $\epsilon$. The scaled equation (6) becomes

$$\begin{aligned} & i\epsilon \frac{\partial \phi^\epsilon}{\partial t} + \frac{\epsilon^2}{2}\Delta\phi^\epsilon - (V(t,\mathbf{x}) + \sqrt{\epsilon}V_1(\frac{\mathbf{x}}{\epsilon}))\phi^\epsilon = 0 \\ & \phi^\epsilon(0,\mathbf{x}) = \phi_0(\frac{\mathbf{x}}{\epsilon},\mathbf{x}). \end{aligned} \tag{43}$$

To describe the passage from (43) to the transport equation in its simplest form we will set $V(t,\mathbf{x}) = 0$. A smooth and $\epsilon$ independent potential $V(t,\mathbf{x})$ that is not zero will not change the scattering terms in the phase space transport equation. It will only affect the Liouville part, in the linear case. Now (27) for $W^\epsilon$ has the form

$$\frac{\partial W^\epsilon}{\partial t} + \mathbf{k}\cdot\nabla_{\mathbf{x}} W^\epsilon + \frac{1}{\sqrt{\epsilon}}\mathcal{L}_{\frac{\mathbf{x}}{\epsilon}} W^\epsilon = 0 \tag{44}$$

where the operator $\mathcal{L}_{\frac{\mathbf{x}}{\epsilon}}$, a rescaled form of (28), is given by

$$\mathcal{L}_{\frac{\mathbf{x}}{\epsilon}} Z(\mathbf{x},\mathbf{k}) = i\int e^{-i\mathbf{p}\cdot\mathbf{x}/\epsilon}\hat{V}_1(\mathbf{p})\left(Z(\mathbf{x},\mathbf{k}+\frac{\mathbf{p}}{2}) - Z(\mathbf{x},\mathbf{k}-\frac{\mathbf{p}}{2})\right)d\mathbf{p}. \tag{45}$$

The behavior of this operator as $\epsilon \to 0$ is very different from (29) when $V_1$ is slowly varying. We can find the correct results by a formal multiscale analysis [14].

Let $\mathbf{y} = \mathbf{x}/\epsilon$ be a fast space variable (on the scale of the wavelength) and introduce an expansion of $W^\epsilon$ of the form

$$W^\epsilon(t,\mathbf{x},\mathbf{k}) = W(t,\mathbf{x},\mathbf{k}) + \epsilon^{1/2}W^{(1)}(t,\mathbf{x},\mathbf{y},\mathbf{k}) + \epsilon W^{(2)}(t,\mathbf{x},\mathbf{y},\mathbf{k}) + \dots, \tag{46}$$

with $\mathbf{y} = \mathbf{x}/\epsilon$ on the right. We assume that the leading term does not depend on the fast scale and that the initial Wigner distribution $W^\epsilon(0,\mathbf{x},\mathbf{k})$ tends to a smooth function $W_0(\mathbf{x},\mathbf{k})$ which is decaying fast enough at infinity. Then the average of the Wigner distribution, $\langle W^\epsilon\rangle$, is close to $W$ which satisfies the transport equation

$$\begin{aligned} & \frac{\partial W}{\partial t} + \mathbf{k}\cdot\nabla_{\mathbf{x}} W - \nabla_{\mathbf{x}} V\cdot\nabla_{\mathbf{k}} W = \overline{\mathcal{L}} W \\ & W(0,\mathbf{x},\mathbf{k}) = W_0(\mathbf{x},\mathbf{k}), \end{aligned} \tag{47}$$

where we have inserted on the left the term due to the potential $V$ in (33). The linear operator $\overline{\mathcal{L}}$ is given by

$$\overline{\mathcal{L}} W(\mathbf{x},\mathbf{k}) = 4\pi\int_{R^3}\hat{R}(\mathbf{p}-\mathbf{k})\delta(\mathbf{k}^2-\mathbf{p}^2)[W(\mathbf{x},\mathbf{p}) - W(\mathbf{x},\mathbf{k})]d\mathbf{p}. \tag{48}$$

The left side of equation (47) has precisely the form (30) of the Liouville equation. The right side is the linear transport operator with differential scattering cross-section $\sigma(\mathbf{k},\mathbf{k}')$ given by

$$\sigma(\mathbf{k},\mathbf{p}) = 4\pi\hat{R}(\mathbf{p}-\mathbf{k})\delta(\mathbf{k}^2-\mathbf{p}^2) \tag{49}$$

and total scattering cross-section $\Sigma(\mathbf{k})$ given by

$$\Sigma(\mathbf{k}) = 4\pi \int_{R^3} \hat{R}(\mathbf{k}-\mathbf{p})\delta(\mathbf{k}^2 - \mathbf{p}^2)d\mathbf{p}. \tag{50}$$

Note also that the transport equation (47) has two important properties. First, the total energy

$$E(t) = \iint_{R^3\times R^3} W(t,\mathbf{x},\mathbf{k})d\mathbf{k}d\mathbf{x} \tag{51}$$

is conserved and second, the positivity of the solution $W(t,\mathbf{x},\mathbf{k})$ is preserved, that is, if the initial Wigner distribution $W_0(\mathbf{x},\mathbf{k})$ is non-negative then $W(t,\mathbf{x},\mathbf{k}) \geq 0$ for $t > 0$.

The physical meaning of the transport approximation for the linear Schrödinger equation with random potential is this. The characteristic wavelength introduced by the initial data is comparable with the scale of the inhomogeneities of the random potential. When we observe the wave energy far from the source and after a long time, it appears to evolve in phase space according to a radiative transport equation with a mean free path that is comparable to the distance from the source of the waves. This kind of behavior is captured with the $\epsilon$ scaling that we have introduced. The scaling of the size of the fluctuations by $\sqrt{\epsilon}$ is introduced so that the mean free path between macroscopic scatterings is comparable to the propagation distance.

The mathematical analysis of the passage from waves to transport in the linear case is considered in [2], [3], [8] and [16]. The paper of Ho, Landau and Wilkins [8] has extensive references and the paper of Erdos and Yau [3] gives a result that is global in time.

In the nonlinear case the potential $V(t,\mathbf{x}) = V^\epsilon(t,\mathbf{x})$ in (43) depends on the solution. In terms of the Wigner function, the potential is $\beta\rho^\epsilon(t,\mathbf{x}) + V_0(\mathbf{x})$ with $\rho^\epsilon = \int W^\epsilon d\mathbf{k}$. We will make a **mean field** hypothesis here, which says that in the transport limit $\epsilon \to 0$ the nonlinear potential keeps its form in the transport equation (47). This amounts to assuming that $\rho^\epsilon \to \rho$ in a strong sense. Some evidence for this is provided in the appendix. However, the mean field hypothesis is very difficult to prove. It is also difficult to test numerically, since the fact that we are in three dimensions is expected to play an important role. There are no mathematical results that deal with the mean field approximation.

**5.1. A linear stability analysis.** Let $\boldsymbol{\xi}$ be the unit vector in the direction of $\mathbf{k}$, i.e., $\mathbf{k} = k\boldsymbol{\xi}$ where $k = |\mathbf{k}|$. For simplicity, in the sequel of the paper we assume that the power spectral density of the inhomogeneities is

$$\hat{R} = \alpha/2\pi$$

with $\alpha$ is a constant. Then (47)-(48) can be written as

$$\partial_t W + \mathbf{k}\cdot\nabla_{\mathbf{x}} W - \nabla_{\mathbf{x}} V \cdot \nabla_{\mathbf{k}} W = \alpha \int\limits_{|\boldsymbol{\xi}'|=1} W(t,\mathbf{x},k,\boldsymbol{\xi}')d\boldsymbol{\xi}' - 4\pi\alpha W, \tag{52}$$

with

$$V = \beta\rho \quad \text{and} \quad \rho = \int_{R^3} W d\mathbf{k}. \tag{53}$$

The initial condition (31) is now rewritten as

$$W(0,\mathbf{x},k,\boldsymbol{\xi}) = \frac{1}{4\pi k^2}\delta\left(k - |\nabla S_0(\mathbf{x})|\right)\delta\left(\boldsymbol{\xi} - \frac{\nabla S_0(\mathbf{x})}{|\nabla S_0(\mathbf{x})|}\right)|A_0(\mathbf{x})|^2. \tag{54}$$

In order to carry out a linear stability analysis we first take the first two moments of (52). Multiplying (52) by 1 and $\mathbf{k}$ respectively and integrating over $\mathbf{k}$, we have

$$\partial_t \rho + \nabla_{\mathbf{x}} \cdot \rho\mathbf{u} = 0 \tag{55}$$

$$\partial_t \rho\mathbf{u} + \nabla_{\mathbf{x}} \cdot \int \mathbf{k}\mathbf{k}W\, d\mathbf{k} - \int \mathbf{k}\nabla_{\mathbf{x}} V \cdot \nabla_{\mathbf{k}} W\, d\mathbf{k} = -4\pi\alpha\rho\mathbf{u}\,. \tag{56}$$

Thus the random inhomogeneity contributes a damping effect. Of course these equations are not closed since high moments are undefined. However they can be used in the linear stability analysis.

First we note that

$$\rho_0 \equiv \bar{\varrho}\,, \quad u_0 \equiv 0\,, \qquad W_0 \equiv \delta(\mathbf{k})\bar{\varrho}\,,$$

with $\bar{\varrho}$ a constant, is a solution of the moment equations (55)-(56). We look for a solution near these constant states, in the form

$$\rho = \overline{\rho} + \rho^{(1)}\,, \qquad \mathbf{u} = \mathbf{u}^{(1)}\,, \tag{57}$$

where

$$\rho^{(1)} << \overline{\rho}\,, \qquad |\mathbf{u}^{(1)}| << 1\,. \tag{58}$$

We also set

$$W = \delta(\mathbf{k} - \mathbf{u})\rho\,. \tag{59}$$

With this ansatz the moment equations can be closed to give

$$\partial_t \rho^{(1)} + \nabla_{\mathbf{x}} \cdot \rho\mathbf{u}^{(1)} = 0 \tag{60}$$

$$\partial_t \rho\mathbf{u}^{(1)} + \nabla_{\mathbf{x}} \cdot \mathbf{u}^{(1)}\mathbf{u}^{(1)}\rho + \beta\rho\nabla_{\mathbf{x}}\rho = -4\pi\alpha\rho\mathbf{u}^{(1)}\,. \tag{61}$$

Using (58) and ignoring higher order terms we obtain the leading order equations

$$\partial_t \rho^{(1)} + \overline{\rho}\nabla_{\mathbf{x}} \cdot \mathbf{u}^{(1)} = 0 \tag{62}$$

$$\partial_t \mathbf{u}^{(1)} + \beta\nabla_{\mathbf{x}}\rho^{(1)} = -4\pi\alpha\mathbf{u}^{(1)}\,. \tag{63}$$

This system is hyperbolic if $\beta \geq 0$ and so is stable in the linear and defocusing cases. However, in the focusing case $\beta < 0$, the system is elliptic. A dispersion relation analysis for (62)-(63) shows that there are three negative eigenvalues

$$-1, \quad -1, \quad -2\pi\alpha - \sqrt{4\pi^2\alpha^2 - \beta\overline{\rho}|\boldsymbol{\eta}|^2}$$

where $\boldsymbol{\eta}$ is the wave number, and a fourth one

$$-2\pi\alpha + \sqrt{4\pi^2\alpha^2 - \beta\overline{\rho}|\boldsymbol{\eta}|^2}\,.$$

This last one is always negative when $\beta > 0$, and zero when $\beta = 0$, suggesting stability in the defocusing and linear cases. It is always negative when $\beta < 0$. The focusing case near uniform solutions with $\mathbf{u} = 0$ is, therefore, linearly unstable.

This means that the only hope for linear stability in the focusing case is to have a nonzero $\mathbf{u}$. This is consistent with the linear stability of the diffusion approximation in the focusing case, which will be derived next.

**6. The parity formulation.** It is convenient to use the parity formulation of the transport equation (47). This allows us to obtain the diffusion approximation in a transparent way.

To get the parity form of (52), we split it into two equations, one for $\mathbf{k}$ and one for $-\mathbf{k}$:

$$\begin{aligned}&\partial_t W(\mathbf{k}) + \mathbf{k}\cdot\nabla_{\mathbf{x}} W(\mathbf{k}) - \nabla_{\mathbf{x}} V\cdot\nabla_{\mathbf{k}} W(\mathbf{k})\\ &\qquad = \alpha \int\limits_{|\boldsymbol{\xi}'|=1} W(t,\mathbf{x},k,\boldsymbol{\xi}')d\boldsymbol{\xi}' - 4\pi\alpha W(\mathbf{k}),\end{aligned} \tag{64}$$

$$\begin{aligned}&\partial_t W(-\mathbf{k}) - \mathbf{k}\cdot\nabla_{\mathbf{x}} W(-\mathbf{k}) + \nabla_{\mathbf{x}} V\cdot\nabla_{\mathbf{k}} W(-\mathbf{k})\\ &\qquad = \alpha \int\limits_{|\boldsymbol{\xi}'|=1} W(t,\mathbf{x},k,\boldsymbol{\xi}')d\boldsymbol{\xi}' - 4\pi\alpha W(-\mathbf{k}).\end{aligned} \tag{65}$$

Define the even and odd parities as

$$\begin{aligned}W^+ &= \frac{1}{2}[W(t,\mathbf{x},\mathbf{k}) + W(t,\mathbf{x},-\mathbf{k})],\\ W^- &= \frac{1}{2}[W(t,\mathbf{x},\mathbf{k}) - W(t,\mathbf{x},-\mathbf{k})].\end{aligned}$$

Adding and subtracting (64) and (65) gives the parity form of the transport equation

$$\partial_t W^+ + \mathbf{k}\cdot\nabla_{\mathbf{x}} W^- - \nabla_{\mathbf{x}} V\cdot\nabla_{\mathbf{k}} W^- = \alpha \int\limits_{|\boldsymbol{\xi}'|=1} W^+(t,\mathbf{x},k,\boldsymbol{\xi}')d\boldsymbol{\xi}' - 4\pi\alpha W^+, \tag{66}$$

$$\partial_t W^- + \mathbf{k}\cdot\nabla_{\mathbf{x}} W^+ - \nabla_{\mathbf{x}} V\cdot\nabla_{\mathbf{k}} W^+ = -4\pi\alpha W^- . \tag{67}$$

The parity formulation has the advantage that the diffusion approximation can be derived easily, as will be shown in the next section.

**7. Nonlinear diffusion limit.** The diffusion approximation is obtained from the parity equations (66) and (67) in the small mean free time limit $1/\alpha \to 0$, and with the time stretched $t \to \alpha t$. Then equation (66) implies that for $\alpha$ large

$$W^+(t,\mathbf{x},\mathbf{k}) = \frac{1}{4\pi} \int\limits_{|\boldsymbol{\xi}'|=1} W^+(t,\mathbf{x},k,\boldsymbol{\xi}')d\boldsymbol{\xi}' \equiv W_0(t,\mathbf{x},k)\,, \tag{68}$$

and so the leading term of $W^+$ is independent of $\boldsymbol{\xi}$. From (67) we have that

$$W^- = -\frac{1}{4\pi\alpha}\left(\mathbf{k}\cdot\nabla_{\mathbf{x}} W_0 - \beta\nabla_{\mathbf{x}}\rho_0\cdot\nabla_{\mathbf{k}} W_0\right), \tag{69}$$

where

$$\rho_0(t,\mathbf{x}) = \int k^2 W_0\, dk$$

and where the time derivative can be neglected on the long-time scale. Using (69) in (66) we get

$$\begin{aligned}&\partial_t W_0 - \mathbf{k}\cdot\nabla_{\mathbf{x}}\frac{1}{4\pi\alpha}\left(\mathbf{k}\cdot\nabla_{\mathbf{x}} W_0 - \beta\nabla_{\mathbf{x}}\rho_0\cdot\nabla_{\mathbf{k}} W_0\right)\\ &\qquad + \beta\nabla_{\mathbf{x}}\rho_0\cdot\nabla_{\mathbf{k}}\frac{1}{4\pi\alpha}\left(\mathbf{k}\cdot\nabla_{\mathbf{x}} W_0 - \beta\nabla_{\mathbf{x}}\rho_0\cdot\nabla_{\mathbf{k}} W_0\right) = 0.\end{aligned} \tag{70}$$

Taking the $\boldsymbol{\xi}$ average $\frac{1}{4\pi}\int_{|\boldsymbol{\xi}|=1} \cdot d\boldsymbol{\xi}$ in (70) yields

$$\begin{aligned}
\frac{\partial W_0}{\partial t} &- \frac{k^2}{4\pi}\frac{1}{4\pi\alpha}\int\limits_{|\boldsymbol{\xi}|=1} \boldsymbol{\xi}\cdot\nabla_{\mathbf{x}}\left(\boldsymbol{\xi}\cdot\nabla_{\mathbf{x}}W_0\right)d\boldsymbol{\xi} + \beta\frac{1}{4\pi}\frac{k}{4\pi\alpha}\int\limits_{|\boldsymbol{\xi}|=1} \boldsymbol{\xi}\cdot\nabla_{\mathbf{x}}\left(\nabla_{\mathbf{x}}\rho_0\cdot\nabla_{\mathbf{k}}W_0\right)d\boldsymbol{\xi} \\
&+\beta\frac{1}{4\pi\alpha}\nabla_{\mathbf{x}}\rho_0\cdot\frac{1}{4\pi}\int\limits_{|\boldsymbol{\xi}|=1}\nabla_{\mathbf{k}}\left(\mathbf{k}\cdot\nabla_{\mathbf{x}}W_0\right)d\boldsymbol{\xi} \\
&-\frac{\beta^2}{4\pi}\nabla_{\mathbf{x}}\rho_0\cdot\frac{1}{4\pi\alpha}\int\limits_{|\boldsymbol{\xi}|=1}\nabla_{\mathbf{k}}\left(\nabla_{\mathbf{x}}\rho_0\cdot\nabla_{\mathbf{k}}W_0\right)d\boldsymbol{\xi} = 0\,.
\end{aligned} \tag{71}$$

By straightforward manipulations (71) becomes

$$\begin{aligned}
\alpha\frac{\partial W_0}{\partial t} &- \frac{1}{12\pi}k^2\Delta W_0 + \beta\frac{k}{12\pi}\nabla_{\mathbf{x}}\cdot\left(\frac{\partial W_0}{\partial k}\nabla_{\mathbf{x}}\rho_0\right) \\
&+\beta\frac{1}{12\pi}\nabla_{\mathbf{x}}\rho_0\cdot\left[\nabla_{\mathbf{x}}\frac{\partial}{\partial k}(kW_0) + 2\nabla_{\mathbf{x}}W_0\right] \\
&-\frac{\beta^2}{12\pi}|\nabla_{\mathbf{x}}\rho_0|^2\left[\frac{\partial^2 W_0}{\partial k^2} + \frac{2}{k}\frac{\partial W_0}{\partial k}\right] = 0\,.
\end{aligned} \tag{72}$$

This is the diffusion approximation of the transport equation (52) and it can also be written in the form

$$\begin{aligned}
\alpha\frac{\partial W_0}{\partial t} &- \frac{1}{12\pi}\begin{pmatrix}\nabla_{\mathbf{x}} \\ \frac{\partial}{\partial k}\end{pmatrix}\cdot\begin{pmatrix}k^2 I_3 & -\beta k\nabla_{\mathbf{x}}\rho_0 \\ -\beta k\left(\nabla_{\mathbf{x}}\rho_0\right)^T & \beta^2|\nabla_{\mathbf{x}}\rho_0|^2\end{pmatrix}\begin{pmatrix}\nabla_{\mathbf{x}}W_0 \\ \frac{\partial W_0}{\partial k}\end{pmatrix} \\
&+\beta\frac{1}{6\pi}\nabla_{\mathbf{x}}\rho_0\cdot\nabla_{\mathbf{x}}W_0 - \frac{\beta^2}{6\pi k}|\nabla_{\mathbf{x}}\rho_0|^2\frac{\partial W_0}{\partial k} = 0\,.
\end{aligned} \tag{73}$$

Here $I_3$ is the $3\times 3$ identity matrix. The diffusion coefficient matrix in (73) is

$$D = \frac{1}{12\pi}\begin{pmatrix}k^2 I_3 & -\beta k\nabla_{\mathbf{x}}\rho_0 \\ -\beta k(\nabla_{\mathbf{x}}\rho_0)^T & \beta^2|\nabla_{\mathbf{x}}\rho_0|^2\end{pmatrix} \tag{74}$$

and it is symmetric and nonnegative semi-definite. However, since $\det D = 0$, the diffusion matrix is degenerate. This is because the scattering operator in (48) is concentrated on the unit sphere. The derivation of the nonlinear diffusion equation (73) is the main result of this paper.

The diffusion equation (72), or (73), can be rewritten into a very simple form [1]. Let

$$e = \frac{k^2}{2}\,, \qquad \tilde{\nabla} = \nabla_{\mathbf{x}} - \beta\nabla_{\mathbf{x}}\rho\,\frac{\partial}{\partial e}, \tag{75}$$

then (72) becomes

$$12\pi\alpha\frac{\partial W_0}{\partial t} - \tilde{\nabla}\cdot\left(2e\tilde{\nabla}W_0\right) + \beta\nabla_{\mathbf{x}}\rho_0\cdot\tilde{\nabla}W_0 = 0\,. \tag{76}$$

We can get equations for moments of $W_0$ which, however, are not closed. First we multiply (72) by $k^2$, integrate over $k$ and then integrate by parts to get

$$12\pi\alpha\frac{\partial\rho_0}{\partial t} - 3\beta\nabla_{\mathbf{x}}\cdot(\rho_0\nabla_{\mathbf{x}}\rho_0) = -\Delta\int k^4 W_0\,dk\,. \tag{77}$$

This gives mass conservation

$$\frac{\partial}{\partial t}\int \rho_0(t,\mathbf{x})\,d\mathbf{x} = 0\,.$$

Let $u_0$ be given by

$$u_0 = \frac{1}{\rho_0}\int k^3 W_0(t,\mathbf{x}\,k)\,dk\,. \tag{78}$$

To get an equation for the second moment we multiply (72) by $k^3$ and integrate over $k$. After integrating by parts we obtain

$$\begin{aligned}\frac{\partial \rho_0 u_0}{\partial t} - \Delta\int k^5 W_0\,dk - 4\beta\nabla_{\mathbf{x}}\cdot(\rho_0 u_0\nabla_{\mathbf{x}}\rho_0) - \beta\nabla_{\mathbf{x}}\rho_0\cdot\nabla_{\mathbf{x}}\rho_0 u_0 \\ -2\beta^2|\nabla_{\mathbf{x}}\rho_0|^2\int kW_0\,dk = 0\,.\end{aligned} \tag{79}$$

Note that equations (77) and (79) are not closed since they involve higher $k$ moments of $W_0$.

As in the usual diffusion theory of the transport equation, an initial layer analysis gives the initial condition for $W_0$ as

$$W_0(0,\mathbf{x},k) = \frac{1}{k^2}\delta\left(k - |\nabla S_0(\mathbf{x})|\right)|A_0(\mathbf{x})|^2\,. \tag{80}$$

**8. Linear stability condition for the nonlinear diffusion equation.** In this section we carry out a linear stability analysis on the diffusion equation (72). This stability analysis gives a simplified but clear picture of how the nonlinear and random effects interact.

We use the moment equations (77) and (79) for the stability analysis. First we note that

$$\rho_0 \equiv \bar{\varrho}\,,\quad u_0 \equiv \overline{u}\,,\qquad W_0 \equiv \frac{1}{k^2}\delta(k-\overline{u})\bar{\varrho}\,,$$

where $\bar{\varrho},\overline{u}$ are constants, is a solution of the moment equations (77) and (79). We look for a solution near these constant states, in the form

$$\rho_0 = \overline{\rho} + \rho^{(1)}\,,\qquad u_0 = \overline{u} + u^{(1)}\,, \tag{81}$$

where

$$\rho^{(1)} << \overline{\rho}\,,\qquad u^{(1)} << \overline{u}\,.$$

We also set

$$W_0 = \frac{1}{k^2}\delta(k-u_0)\rho_0\,. \tag{82}$$

With this ansatz the moment equations can be closed to give

$$12\pi\alpha\frac{\partial\rho_0}{\partial t} - \Delta\rho_0 u_0^2 - 3\beta\nabla_{\mathbf{x}}\cdot(\rho_0\nabla_{\mathbf{x}}\rho_0) = 0\,. \tag{83}$$

$$\begin{aligned}12\pi\alpha\frac{\partial\rho_0 u_0}{\partial t} - \Delta\rho_0 u_0^3 - 4\beta\nabla_{\mathbf{x}}\cdot(\rho_0 u_0\nabla_{\mathbf{x}}\rho_0) \\ -\beta\nabla_{\mathbf{x}}\rho_0\cdot\nabla_{\mathbf{x}}\rho_0 u_0 - 2\beta^2|\nabla_{\mathbf{x}}\rho_0|^2\frac{\rho_0}{u_0} = 0\,.\end{aligned} \tag{84}$$

With the linearization (81), the last two terms in (84) are insignificant and so will be neglected. The moment equations thus become

$$12\pi\alpha\frac{\partial\rho_0}{\partial t} - \Delta\rho_0 u_0^2 - 3\beta\nabla_{\mathbf{x}}\cdot(\rho_0\nabla_{\mathbf{x}}\rho_0) = 0\,, \tag{85}$$

$$12\pi\alpha\frac{\partial\rho_0 u_0}{\partial t} - \Delta\rho_0 u_0^3 - 4\beta\nabla_{\mathbf{x}}\cdot(\rho_0 u_0\nabla_{\mathbf{x}}\rho_0) = 0\,. \tag{86}$$

We now do the linearization (81) and, keeping only the leading terms, obtain the coupled system of linear diffusion equations

$$12\pi\alpha\frac{\partial\rho_1}{\partial t} = (\overline{u}^2 + 3\beta\overline{\varrho})\Delta\rho_1 + 2\overline{\varrho}\overline{u}\Delta u_1\,, \tag{87}$$

$$12\pi\alpha\frac{\partial u_1}{\partial t} = \beta\overline{u}\Delta\rho_1 + \overline{u}^2\Delta u_1\,. \tag{88}$$

**8.1. Linear stability from the diffusion matrix.** The diffusion coefficient matrix of (87) and (88)

$$A = \begin{pmatrix} \overline{u}^2 + 3\beta\overline{\varrho} & 2\overline{\varrho}\overline{u} \\ \beta\overline{u} & \overline{u}^2 \end{pmatrix} \tag{89}$$

has two eigenvalues

$$\lambda_\pm = \overline{u}^2 + \frac{3}{2}\beta\overline{\varrho} \pm \frac{1}{2}\sqrt{8\beta\overline{\varrho}\overline{u}^2 + 9\beta^2\overline{u}^2}\,. \tag{90}$$

Clearly, $Re(\lambda_\pm) > 0$ if and only if

$$\overline{u}^2 + \frac{3}{2}\beta\overline{\varrho} > 0\,. \tag{91}$$

This means that the right side of the variance identity (4) in the high frequency limit, where $H$ has the form (12) or (17) in the $\rho,\ \mathbf{u}$ variables, must be positive for stability. Therefore, even in the focusing case $\beta < 0$, the initial value problems for the linear diffusion equations (87) and (88) are well posed as long as (91) is satisfied,

It is surprising that the stability condition (91) does not depend on the strength $\alpha$ of the random inhomogeneities, although the diffusion rate does. It is also surprising that the right side of the variance identity comes up as a **stability** condition, while in the analysis of the NLS equation it is used to get focusing solutions (instability) when (5) is negative.

**8.2. Linear stability for the energy.** We now study the stability of (87)-(88) in the energy norm. In the linear case when $\beta = 0$, it is obvious that (87)-(88) is stable. We analyze the defocusing and focusing cases separately.

In the defocusing case, $\beta > 0$, we multiply (87) by $\beta\rho$, and (88) by $\bar{\varrho}u$, then add the resulting equations and integrate over $\mathbf{x}$. Upon integration by parts, we obtain

$$\begin{aligned} 12\pi\alpha\frac{\partial}{\partial t}\int\left(\frac{\beta}{2}\rho^2 + \frac{1}{2}\bar{\varrho}u^2\right)d\mathbf{x} &= -\int\beta(\overline{u}^2 + 3\beta\overline{\varrho})|\nabla\rho|^2 + 3\beta\overline{\varrho}\overline{u}\nabla\rho\cdot\nabla u + \overline{\varrho}\overline{u}^2|\nabla u|^2\,d\mathbf{x} \\ &= -\int\beta(\overline{u}^2 + \frac{3}{4}\beta\overline{\varrho})|\nabla\rho|^2\,d\mathbf{x} \\ &\quad -\int\frac{9}{4}\beta^2\overline{\varrho}|\nabla\rho|^2 + 3\beta\overline{\varrho}\overline{u}\nabla\rho\cdot\nabla u + \overline{\varrho}\overline{u}^2|\nabla u|^2\,d\mathbf{x} \\ &= -\int\beta(\overline{u}^2 + \frac{3}{4}\beta\overline{\varrho})|\nabla\rho|^2\,d\mathbf{x} - \int\overline{\varrho}|\frac{3}{2}\beta\nabla\rho + \overline{u}\nabla u|^2\,d\mathbf{x} \\ &\le 0\,. \end{aligned} \tag{92}$$

Thus, in the defocusing case the system (87)-(88) is always stable.

In the focusing case, $\beta < 0$, we again multiply (87) by $\beta\rho$, and (88) by $2\bar{\varrho}u$. We then **subtract** the first equation from the second one. By integrating over $\mathbf{x}$ and integrating by parts, we obtain

$$(93)\quad 12\pi\alpha\frac{\partial}{\partial t}\int\left(\bar{\varrho}u^2-\frac{\beta}{2}\rho^2\right)d\mathbf{x} = -2\bar{\varrho}\overline{u}^2\int|\nabla u|^2\,d\mathbf{x}+\beta\int(\overline{u}^2+3\beta\,\bar{\varrho})|\nabla\rho|^2\,d\mathbf{x}\,.$$

Clearly, a sufficient condition for the above term to be non-positive is

$$(94)\qquad \overline{u}^2+3\beta\,\bar{\varrho}\geq 0.$$

This means that the coefficient of $\Delta\rho$ in (87) should be nonnegative, which means that the diagonal entries of the matrix $A$ should be nonnegative.

**9. Numerical solution of the nonlinear transport equation.** In this section we will present some numerical results for the nonlinear transport equation (52)-(53). In order to have good resolution we assume spherical symmetry and use a second order, non-oscillatory, upwind scheme [12]. The solution depends only on $r = |\mathbf{x}|$, $k$ and $\theta = \cos^{-1}\dfrac{\mathbf{x}\cdot\mathbf{k}}{rk}$, the angle between $\mathbf{x}$ and $\mathbf{k}$. In these variables equations (52) and (53) become

$$(95)\qquad \begin{aligned}&\frac{\partial W}{\partial t}+\mathrm{k}\cos\theta\frac{\partial W}{\partial r}-\frac{k}{r}\sin\theta\frac{\partial W}{\partial\theta}-\beta\frac{\partial V}{\partial r}\left(\cos\theta\frac{\partial W}{\partial k}-\frac{\sin\theta}{k}\frac{\partial W}{\partial\theta}\right)\\ &\quad=2\pi\alpha\int_0^\pi W\sin\theta d\theta-4\pi\alpha W,\\ &V=V(\rho)\,,\qquad \rho=\int_0^\infty\int_0^{2\pi}Wk^2\sin\theta dk\,d\theta.\end{aligned}$$

In terms of the direction cosine $-1\leq\mu=\cos\theta\leq 1$, (95) can be rewritten in conservation form as

$$(96)\qquad \begin{aligned}&\frac{\partial W}{\partial t}+\frac{\partial}{\partial r}(\mu kW)+\frac{\partial}{\partial k}\left(-\beta\mu\frac{\partial V}{\partial r}W\right)+\frac{\partial}{\partial\mu}\left[(1-\mu^2)\left(\frac{k}{r}-\frac{\beta}{k}\frac{\partial V}{\partial r}\right)W\right]\\ &\quad=2\pi\alpha\int_{-1}^1 W(t,r,k,\mu')\,d\mu'-4\pi\alpha W,\\ &V=V(\rho)\,,\qquad \rho=\int_0^\infty\int_{-1}^1 Wk^2dkd\mu,\end{aligned}$$

where $W = W(t,r,k,\mu)$. The initial condition for (96) is

$$(97)\qquad W(0,r,k,\mu)=\frac{1}{k^2}\delta(k-u_0(r))\,\delta(\mu-a_0(r))\rho_0(r).$$

**9.1. The numerical method.** We will use a second order upwind scheme for spatial discretizations. This is a natural choice since (96) is a hyperbolic equation. We use the composite midpoint rule for angular integration and the second order explicit Runge-Kutta method for time discretization. The overall accuracy is of second order.

Let $r_{i+1/2}(0 \le i \le I)$ be the grid points in the $r$-direction, and likewise define $k_{j+1/2}(0 \le j \le J)$ and $\mu_{l+1/2}(0 \le l \le L)$. Let $r_i, k_j, \mu_l$ be the midpoints (for example $r_i = \frac{1}{2}(r_{i+1/2} + r_{i-1/2})$). Let $\Delta r = r_{i+1/2} - r_{i-1/2}$, $\Delta k = k_{j+1/2} - k_{j-1/2}$ and $\Delta \mu = \mu_{l+1/2} - \mu_{l-1/2}$ be the uniform grid sizes in each direction. Let $W_{ijl}$ be the numerical approximation of $W$ at $(r_i, k_j, \mu_l)$, and $W_{i+1/2,j,l}$ be the approximation of $W$ at $(r_{i+1/2}, s_j, \mu_l)$. We define $W_{i,j+1/2,l}$ and $W_{ij,l+1/2}$ in a similar way. A second order conservative approximation for (96) is

$$
\begin{aligned}
(98)\quad \frac{\partial}{\partial t} W_{ijl} &+ \frac{\mu_l k_j}{\Delta r}(W_{i+1/2,j,l} - W_{i-1/2,j,l}) - \frac{\mu_l}{\Delta k}\frac{\partial V_i}{\partial r}(W_{i,j+1/2,l} - W_{i,j-1/2,l}) \\
&+ \frac{1-\mu_l^2}{\Delta \mu}\left(\frac{k_j}{r_i} - \frac{1}{k_j}\frac{\partial V_i}{\partial r}\right)(W_{i,j,l+1/2} - W_{i,j,l-1/2}) \\
&= 2\pi\alpha \int_{-1}^{1} W_{ij}\,(t,r,k,\mu') - 4\pi\alpha W_{ijl}.
\end{aligned}
$$

To get the flux $W_{i+1/2,jl}$ from the known quantity $W_{ijl}$ we use the second order upwind scheme due to van Leer [12]

$$
(99)\qquad W_{i+1/2,jl} = W_{ijl} + \frac{\Delta r}{2}\sigma_i^r\,, \qquad \text{if} \quad \mu_l > 0\,;
$$

$$
(100)\qquad W_{i+1/2,jl} = W_{i+1,jl} - \frac{\Delta r}{2}\sigma_{i+1}^r\,, \qquad \text{if} \quad \mu_l < 0\,.
$$

Here $\sigma_i^r$ is the limited slope [12]

$$
(101)\qquad \sigma_i^r = \frac{1}{\Delta r}(W_{i+1,jl} - W_{ijl})\phi(\theta^r)
$$

$$
(102)\qquad \theta^r = \frac{W_{ijl} - W_{i-1,jl}}{W_{i+1,jl} - W_{ijl}}
$$

$$
(103)\qquad \phi(\theta) = \frac{|\theta| + \theta}{1 + |\theta|}\,,
$$

A limited slope scheme is necessary, especially for the defocusing case, since moments of the nonlinear transport equation are close to the gas dynamics equations. Without a limited slope the numerical solutions become oscillatory when shocks develop. We define the flux in the $k$-direction in a similar way

$$
(104)\qquad W_{i,j+1/2,l} = W_{ijl} + \frac{\Delta k}{2}\sigma_j^k\,, \qquad \text{if} \quad -\mu_l\frac{\partial V_i}{\partial r} > 0\,;
$$

$$
(105)\qquad W_{i,j+1/2,l} = W_{i,j+1,l} - \frac{\Delta k}{2}\sigma_{j+1}^k\,, \qquad \text{if} \ -\mu_l\frac{\partial V_i}{\partial r} < 0\,,
$$

where $\sigma_i^k$ is defined as in (101). The flux in the $\mu$-direction is given by

$$
(106)\qquad W_{i,j,l+1/2} = W_{ijl} + \frac{\Delta \mu}{2}\sigma_l^\mu\,, \qquad \text{if} \quad \frac{k_j}{r_i} - \frac{1}{k_j}\frac{\partial V}{\partial r} > 0\,;
$$

$$
(107)\qquad W_{i,j,l+1/2} = W_{i,j,l+1} - \frac{\Delta \mu}{2}\sigma_{l+1}^\mu\,, \qquad \text{if} \quad \frac{k_j}{r_i} - \frac{1}{k_j}\frac{\partial V}{\partial r} < 0\,,
$$

where $\sigma_l^\mu$ is defined as in (101).

To find $\frac{\partial V_i}{\partial r}$, given that $V'(r) = V'(\rho)\frac{\partial \rho}{\partial r}$, we need to evaluate $\frac{\partial \rho_i}{\partial r}$. We use the centered difference

$$
\begin{aligned}
(108) \qquad \frac{\partial \rho_i}{\partial r} &\approx \frac{\rho_{i+1/2} - \rho_{i-1/2}}{\Delta r} \\
&= \frac{1}{\Delta r}\left(\int_0^\infty \int_{-1}^1 W_{i+1/2}(t,k,\mu)dkd\mu - \int_0^\infty \int_{-1}^1 W_{i-1/2}(t,k,\mu)dkd\mu\right) \\
&\approx \frac{\Delta k \Delta \mu}{\Delta r}\sum_{j,l}(W_{i+1/2,j,l} - W_{i-1/2,j,l}).
\end{aligned}
$$

Here we have used the composite midpoint rule to approximate the integral. It has second order accuracy in $k$ and $\mu$. We can use the flux $W_{i+1/2,j,l}$ already obtained from (100) in (108). To recover $V_{i+1/2}$ we use the integral

$$
(109) \qquad \rho_{i+1/2} = \rho_{1/2} + \int_0^{r_{i+1/2}} \frac{\partial \rho}{\partial r} dr \approx \rho_{1/2} + \sum_{j=0}^{i} \frac{\partial \rho_j}{\partial r}\Delta r
$$

where the composite midpoint rule has again been used.

**Time discretization:** We use the second order Runge-Kutta method.

**Boundary conditions:** Since the numerical flux has a five point stencil it is necessary to have two fictitious points outside the physical boundaries. To define $W$ on the left of $r = 0$ we use the condition

$$
(110) \qquad W(t,-r,k,\mu) = W(t,r,k,-\mu).
$$

This makes sense physically because equation (96) remains unchanged if we replace $r$ by $-r$ and $\mu$ by $-\mu$ simultaneously. To define $W$ to the left of $k = 0$ we use a similar condition

$$
(111) \qquad W(t,r,-k,\mu) = W(t,r,k,-\mu).
$$

The scattering term in (96) is small near $k = 0$. At outer boundaries of $r$ and $k$ we use outgoing boundary conditions. For the computations the domain in $k$ is large enough so that at the outer boundary $W$ is nearly zero. At $\mu = \pm 1$ we simply use the reflecting boundary condition $\frac{\partial W}{\partial \mu} = 0$.

More precisely, we fix the numerical boundary conditions at $r = 0$ as follows. If $\frac{\partial V}{\partial r} < 0$ we first extrapolate $W$ to second order for $\mu < 0$ from the interior value of $W$ to get $W_{-1/2,jl}$ and $W_{-2/3,jl}$, where $r_{-1/2} = -r_{1/2}$ and $r_{-3/2} = -r_{3/2}$ are the fictitious points. To obtain $W$ at the fictitious points for $\mu > 0$ we use the condition (110) numerically, i.e., $W_{-1/2.jl} = W_{1/2,j,L-l+1}$ and $W_{-3/2,jl} = W_{3/2,j,L-l+1}$. If $\frac{\partial V}{\partial r} > 0$ we reverse this process. This corresponds to extrapolation in an upwind direction, which is necessary for a hyperbolic equation. At $k = 0$ we impose a similar boundary condition. At the outer boundaries we always assume zero incoming flux and the outgoing flux is simply the outflow boundary condition.

**9.2. Numerical results.** We will now present the results of some numerical experiments for the nonlinear transport equation (96). We want to see the effect of randomness, which in (96) is the scattering term, on the focusing nonlinearity. We use the potential

$$
V(\rho) = \beta\rho.
$$

The initial energy density is

$$W(0,r,k,\mu) = \frac{1}{k^2}\delta(k-1)\delta(\mu)\rho_0(r)\,, \tag{112}$$

but in the numerical computations we use the Gaussian

$$W(0,r,k,\mu) = \frac{\lambda^2}{\pi}\frac{1}{k^2}\, e^{-\lambda^2((k-1)^2+\mu^2)}\rho_0(r) \tag{113}$$

which gives for

$$\rho_0(r) = e^{-\lambda^2 r^2} + 0.5\,. \tag{114}$$

This initial density regularizes the *delta*-function. The smoothing effect of the parameter $\lambda$ is explored numerically below. The nonlinear transport equation with *delta*-function initial data is quite singular and there is no theoretical justification for expecting it to correspond to the limiting behavior $\lambda \to \infty$ of the regularized solutions.

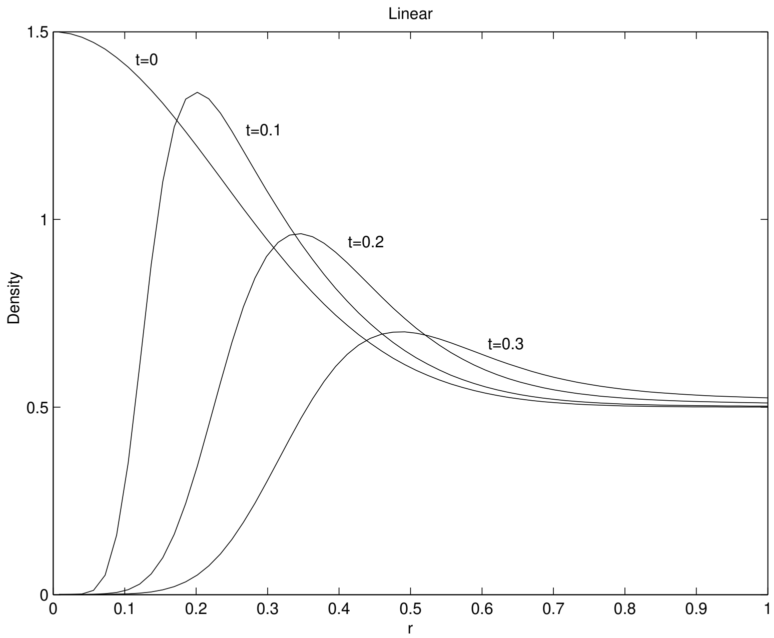


FIG. 1. *The density $\rho(t,r)$ versus $r$ for the linear case without randomness, $(\alpha = \beta = 0)$ and $\lambda = 3$. Note that the energy is propagating away from the origin.*

The computational domain in $r, k, \mu$ space is $[0,2]\times[0,2]\times[-1,1]$. We use 120 cells in $r$, 120 cells in $k$, and 40 cells in $\mu$. We use $\Delta t = 10^{-4}$ for the linear case, $\Delta t = 5\times 10^{-6}$ for the defocusing case, and $\Delta t = 10^{-5}$ for the focusing cases. In the focusing case the solution is less diffusive and the CFL condition allows a slightly larger $\Delta t$ than in the defocusing case. We first use $\lambda = 3$.

1. The linear case ($\beta = 0$). If there is no randomness ($\alpha = 0$), wave energy moves away from the origin, as in Fig. 1. By turning on the random terms ($\alpha = 0.7$) we see that it tends to slow down the spreading of the energy as shown in Fig. 2.

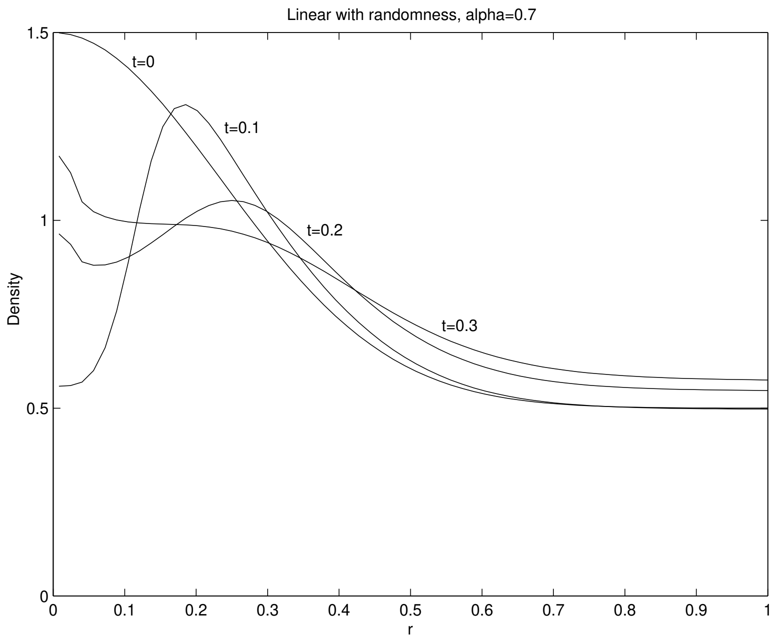


FIG. 2. *The density $\rho(t, r)$ versus $r$ for the linear case with randomness $\alpha = 0.7$ and $\lambda = 3$. Wave energy spreading is slower than that of Fig. 1 without randomness.*

2. The defocusing case ($\beta = 1$). The energy density without randomness ($\alpha = 0$) is shown in Fig. 3. It propagates away from the origin much faster than in the linear case, Fig. 1. In Fig. 4 we show the energy density in the defocusing case with randomness ($\alpha = 0.7$). The solution is more spread out than in the linear case.
3. The focusing case. If there is no randomness ($\alpha = 0$), the numerical solution becomes highly oscillatory (one wave length per grid point), Fig. 5, reflecting the unstable nature of the problem. By turning on the randomness, for example, at $\alpha = 0.7$, numerical results are stable, at least when $|\beta|$ is not too large. We compare the results of $\beta = -0.2$ and $\beta = -0.5$ in Fig. 6 and Fig. 7 respectively. In both cases the solutions spread out slower than in the linear case, and larger $|\beta|$ slows down the spreading of the solution. We also consider the smoothing effect of the initial data. In Fig. 8 and Fig. 9 we compare numerical solutions with $\lambda = 6$ and $\lambda = 9$, respectively. The solutions are quite close to each other. The larger $\lambda$ slows down spreading a bit, but the qualitative behavior of the numerical solutions remains the same.

It still remains an important issue to investigate the quantitative relation among $\alpha, \beta$ and $\lambda$ and how it effects the stability of the physical problem. This will be a topic for future research.

**10. Numerical solution of the nonlinear diffusion equation.** We also solve numerically the nonlinear diffusion equation (72). We rescale the time variable so that $\alpha$ disappears. We have four independent variables but we will assume spherical symmetry to reduce them to two. Let $r = |\mathbf{x}|$, and $W(t, \mathbf{x}, k) = W(t, r, k)$. The

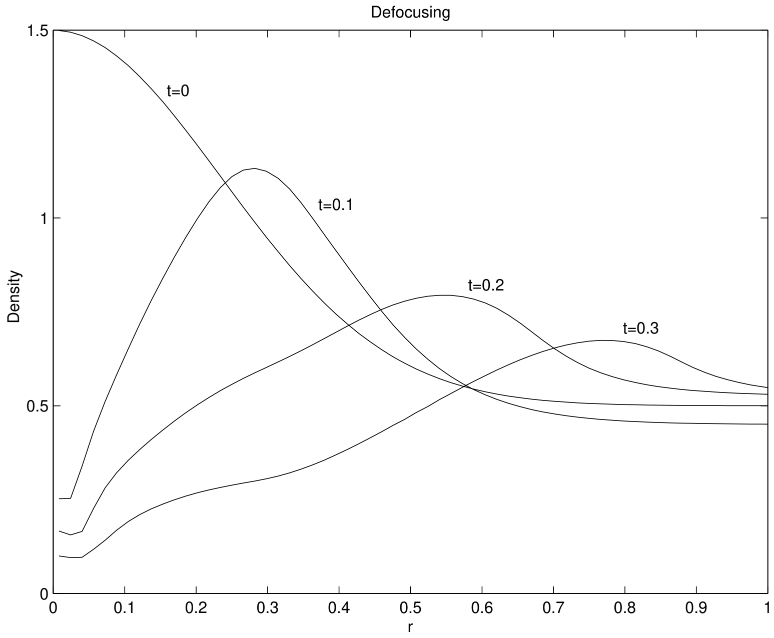


FIG. 3. *The density $\rho(t, r)$ versus $r$ for the defocusing case with no randomness ($\alpha = 0, \beta = 1$) and $\lambda = 3$. The wave energy propagates away from the origin much faster than in the linear case.*

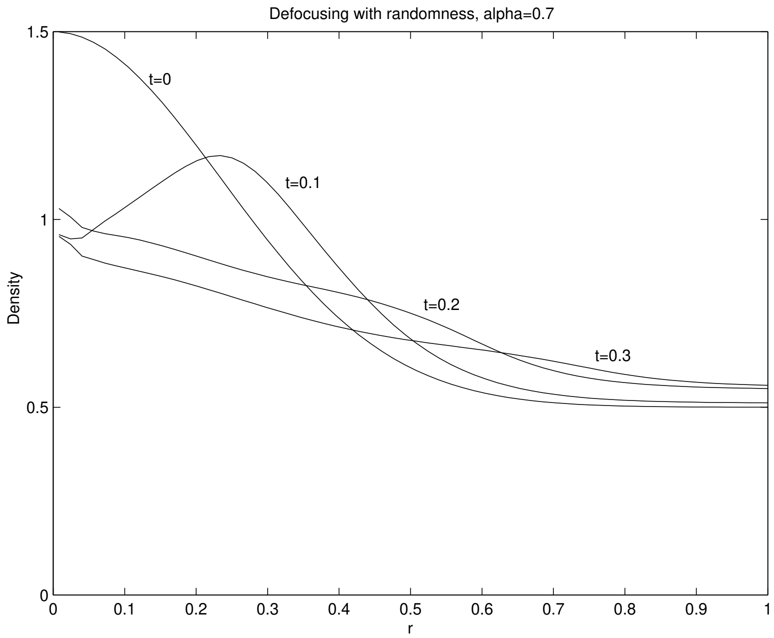


FIG. 4. *The energy density $\rho(t, r)$ versus $r$ in the defocusing case with randomness ($\alpha = 0.7, \beta = 1$) and $\lambda = 3$. The density is more spread out.*

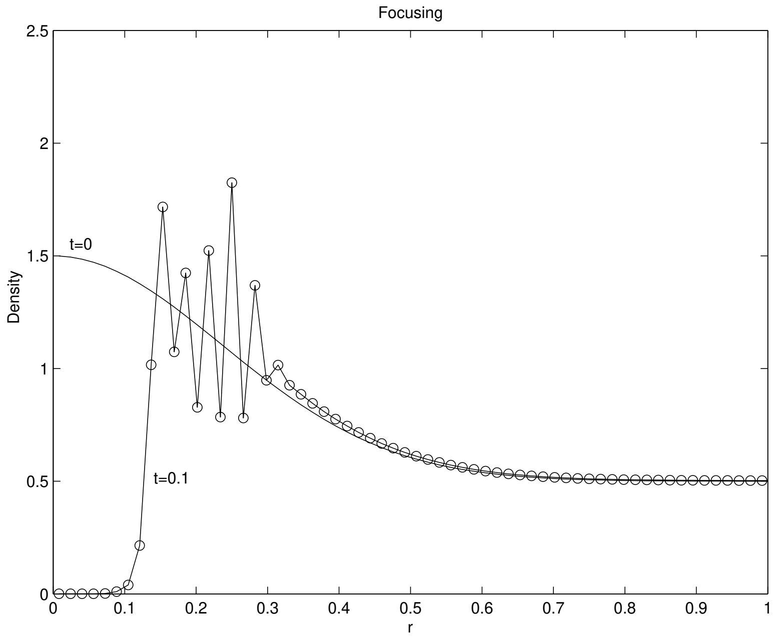


FIG. 5. *The energy density $\rho(t,r)$ versus $r$ for the focusing case with no randomness. Here $\beta = -0.2$ and $\lambda = 3$.*

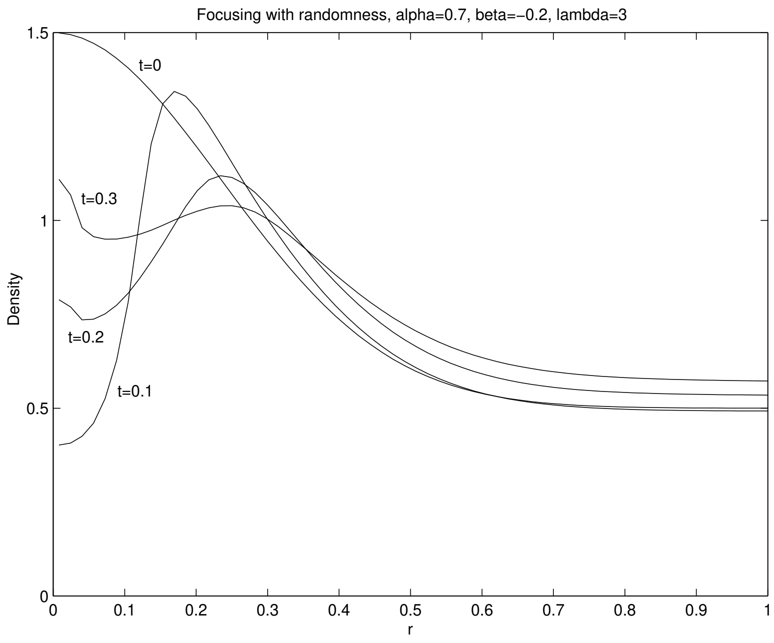


FIG. 6. *The energy density $\rho(t,r)$ versus $r$ for the focusing case with randomness. Here $\alpha = 0.7, \beta = -0.2$ and $\lambda = 3$.*

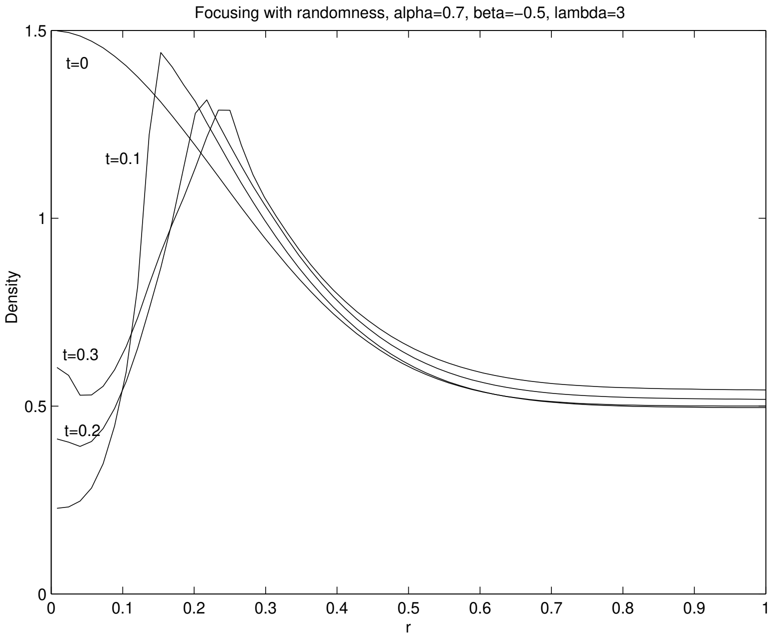


FIG. 7. *The energy density $\rho(t, r)$ versus $r$ for the focusing case with randomness. Here $\alpha = 0.7, \beta = -0.5$ and $\lambda = 3$.*

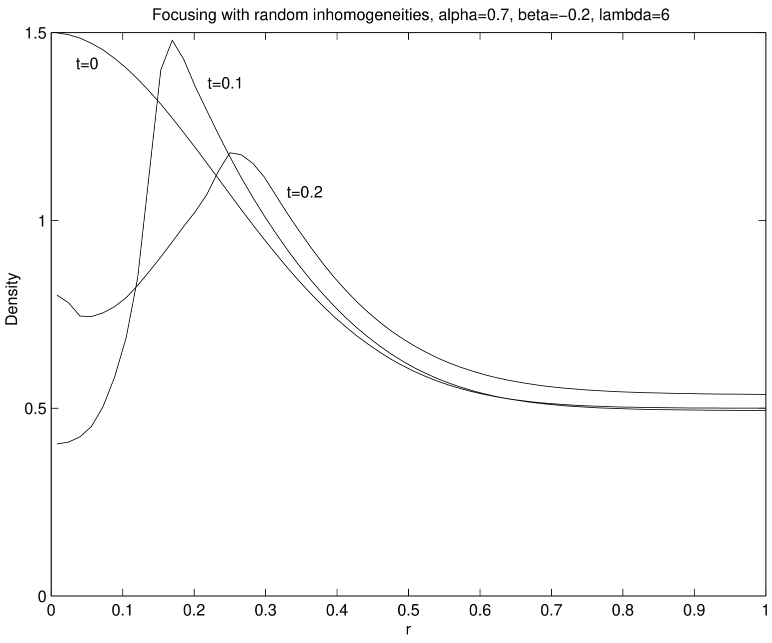


FIG. 8. *The energy density $\rho(t, r)$ versus $r$ for the focusing case with randomness. Here $\alpha = 0.7, \beta = -0.2$ and $\lambda = 6$.*

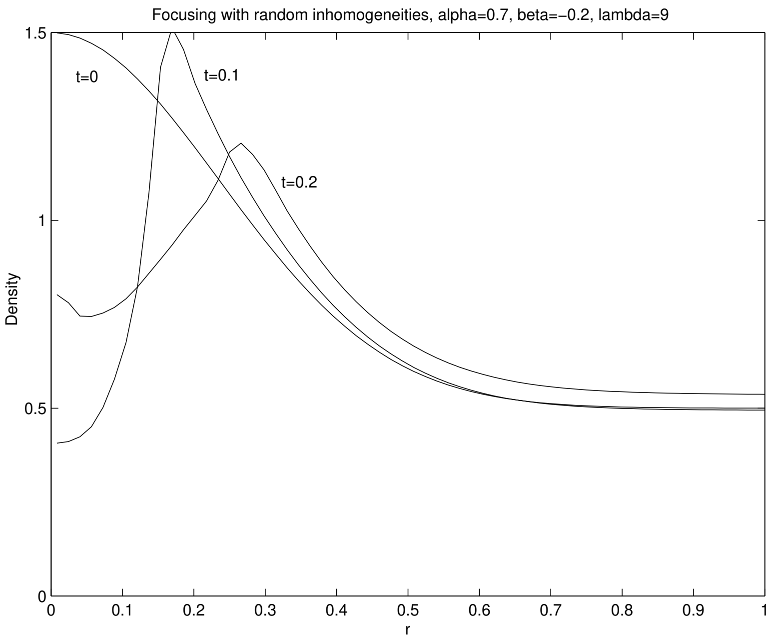


FIG. 9. *The energy density $\rho(t,r)$ versus $r$ for the focusing case with randomness. Here $\alpha = 0.7, \beta = -0.2$ and $\lambda = 9$.*

diffusion equation (72) in polar coordinates is

$$\begin{aligned} &\frac{\partial W_0}{\partial t} - \frac{1}{12\pi}\frac{k^2}{r^2}\frac{\partial}{\partial r}\left(r^2\frac{\partial W_0}{\partial r}\right) + \frac{k}{12\pi}\frac{\partial W_0}{\partial k}\frac{1}{r^2}\frac{\partial}{\partial r}\left(r^2\frac{\partial V}{\partial r}\right) + \frac{k}{6\pi}\frac{\partial^2 W_0}{\partial r \partial k}\frac{\partial V}{\partial r} \\ &\quad + \frac{1}{4\pi}\frac{\partial V}{\partial r}\frac{\partial W_0}{\partial r} - \frac{1}{12\pi}\left(\frac{\partial V}{\partial r}\right)^2\frac{\partial^2 W_0}{\partial k^2} - \frac{1}{6\pi k}\left(\frac{\partial V}{\partial r}\right)^2\frac{\partial W_0}{\partial k} = 0\,, \\ &\qquad V(\rho) = \beta\rho\,, \end{aligned} \tag{115}$$

with the initial condition

$$W_0(0,r,k) = \frac{1}{k^2}\delta\left(k - u_0(r)\right)\rho_0(r). \tag{116}$$

We use a second-order centered difference scheme for spatial derivatives and composite midpoint rule to approximate $\rho_0(r)$. Let $W_{i,j}$ denote the spatial discretization of $W_0$. The spatially discretized form of equation (115) is

$$\begin{aligned} &\frac{\partial W_{i,j}}{\partial t} - \frac{1}{12\pi}\frac{k_j^2}{r_i^2(\Delta r)^2}(r_{i+1/2}^2(W_{i+1,j} - W_{i,j}) - r_{i-1/2}^2(W_{i,j} - W_{i-1,j}) \\ &\quad + \frac{k}{12\pi r_i^2}\frac{W_{i,j+1} - W_{i,j-1}}{2\Delta k}\frac{1}{(\Delta r)^2}[r_{i+1/2}^2(V_{i+1} - V_i) - r_{i-1/2}^2(V_i - V_{i-1})] \\ &\quad + \frac{k_j}{6\pi}\frac{V_{i+1} - V_{i-1}}{2\Delta r}\frac{1}{4\Delta r \Delta k}(W_{i+1,j+1} - W_{i+1,j-1} - W_{i-1,j+1} + W_{i-1,j-1}) \\ &\quad + \frac{1}{4\pi}\frac{V_{i+1} - V_{i-1}}{2\Delta r}\frac{W_{i+1,j} - W_{i-1,j}}{2\Delta r} \end{aligned} \tag{117}$$

$$- \frac{1}{12\pi} \left( \frac{V_{i+1} - V_{i-1}}{2\Delta r} \right)^2 \frac{1}{\Delta k^2} (W_{i,j+1} - 2W_{i,j} + W_{i,j-1})$$
$$- \frac{1}{6\pi k_j} \left( \frac{V_{i+1} - V_{i-1}}{2\Delta r} \right)^2 \frac{W_{i,j+1} - W_{i,j-1}}{2\Delta k} = 0.$$

Here we define $r_{i+1/2} = (r_i + r_{i+1})/2$ and $k_{j+1/2} = (k_j + k_{j+1})/2$. To get $V_i$ from $W$ we use the composite midpoint rule. For time discretization we use the second-order Runge-Kutta method. At $r = 0$ or $k = 0$ we use reflecting boundary conditions. At the outer boundaries we use vanishing flux conditions. It is important to have a domain in $k$ that is large enough so that $W$ is very small at the outer boundary of $k$. We choose the initial data

$$W_0(0, r, k) = \frac{1}{k^2} e^{-9((k-1)^2 + r^2)} \tag{118}$$

The domain of integration is $[0, 1] \times [0, 2]$. We take 32 points in $r$, 64 points in $k$ and $\Delta t = 10^{-4}$. The numerical results for linear, defocusing and focusing (with $\beta = -1$ and $\beta = -0.5$) are shown in Figs. 10,11,12,13, respectively. In the linear case there is less diffusion than in the defocusing case, while in the focusing case diffusion is quite reduced. In fact, in the focusing case with $\beta = -1$ the stability condition (91) is not satisfied in part of the domain and $\rho(t, r)$ grows locally as the solution tends to focus. In Fig. 12 we show the solution until it is about to blow-up (at $t \approx 0.51$). By decreasing $\Delta t$ we may compute the solution to a slightly longer time but it still breaks down numerically. For a stable solution we have to take a smaller $|\beta|$. In Fig 13 we show $\rho$ with $\beta = -0.5$ so that the stability condition (91) is satisfied in the whole domain. The solution is stable and diffuses, at a slower rate than in the linear case. Our numerical results support the linear stability analysis that leads to (91). If (91) holds at every point of the domain initially then the nonlinear diffusion equation is stable in time.

In Fig. 14 we plot the diffusivity

$$\sigma(t) = \int_0^\infty \int_0^\infty W_0 r^4 k^2 \, dr dk \tag{119}$$

as a function of time, where the integrals are computed numerically with the composite midpoint rule. We see more clearly what we observe in the previous figures. The slope of $\sigma(t)$, the rate of diffusion, decreases as we go from the defocusing to the linear and to the focusing ($\beta = -0.5$) case.

**11. Summary and conclusions.** We have studied the interaction of nonlinear waves, solutions of the nonlinear Schrödinger equation (NLS), and random inhomogeneities, which have mean zero, are stationary and have correlation length comparable to the wavelength. Using the Wigner phase space form of the Schrödinger equation, we derive formally a nonlinear, mean field transport approximation in the high frequency limit, and then get the diffusion approximation of this nonlinear transport equation. A linear stability analysis of the nonlinear diffusion equation shows in a simplified way how the nonlinearity and randomness interact. The focusing nonlinearity has an anti-diffusive effect (see (91) with $\beta < 0$) but as long as it is not very strong the diffusion equation is linearly stable. The linear stability condition (91) has a surprising connection with the variance identity of the NLS (4): it is the right side of this identity in the high frequency limit.

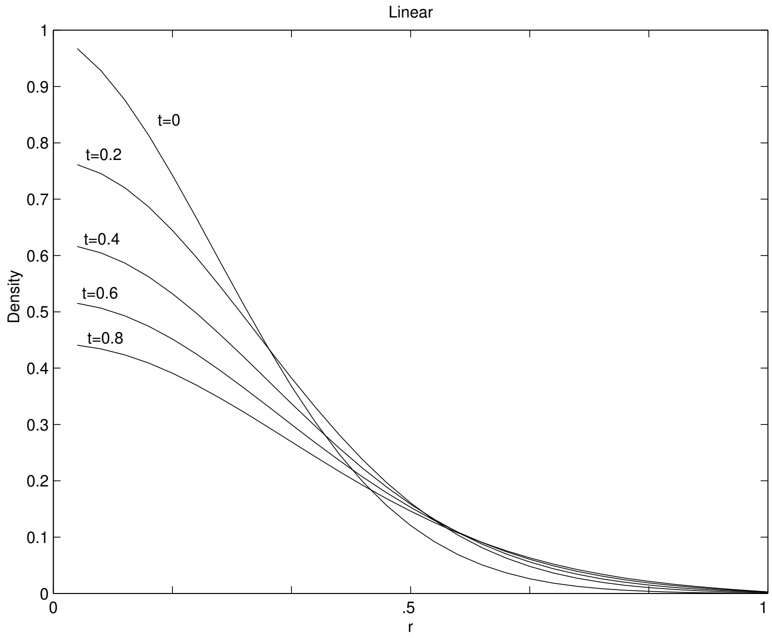


FIG. 10. *The energy density $\rho(t, r)$ in the diffusion approximation in the linear case, plotted as a function of $r$ with $\Delta t = 0.0001$.*

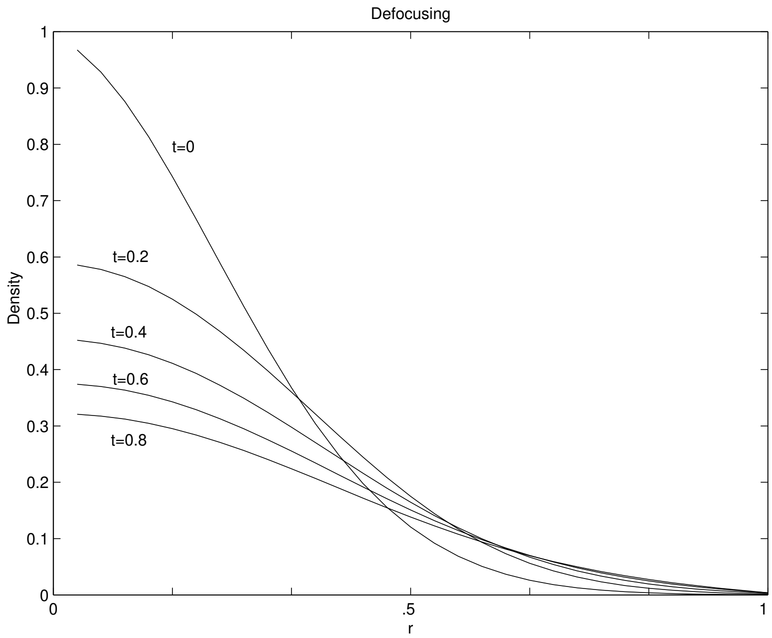


FIG. 11. *The energy density $\rho(t, r)$ in the diffusion approximation in the defocusing case ($\beta = 1$), plotted as a function of $r$ with $\Delta t = 0.0001$.*

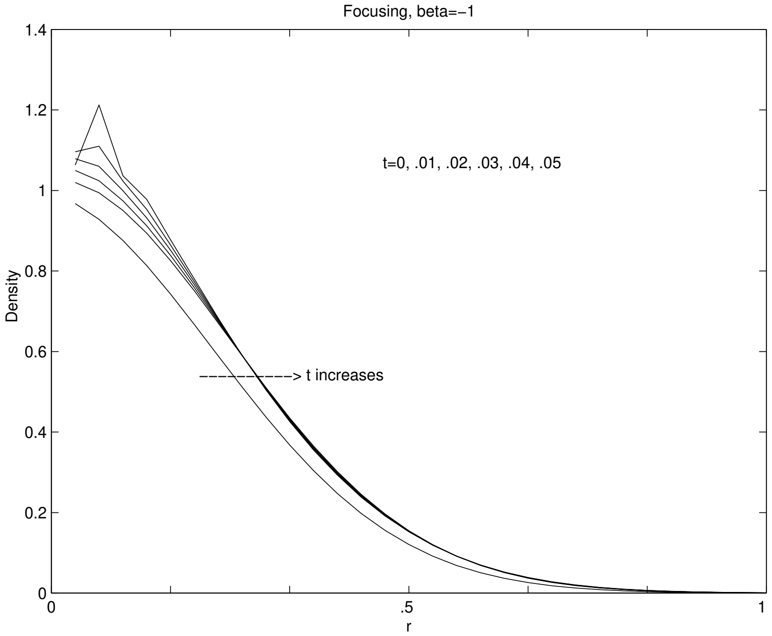


FIG. 12. *The energy density $\rho(t,r)$ in the diffusion approximation in the focusing case with $\beta=-1$, plotted as a function of $r$ with $\Delta t = 0.0001$. Note the onset of instability where condition (91) is violated.*

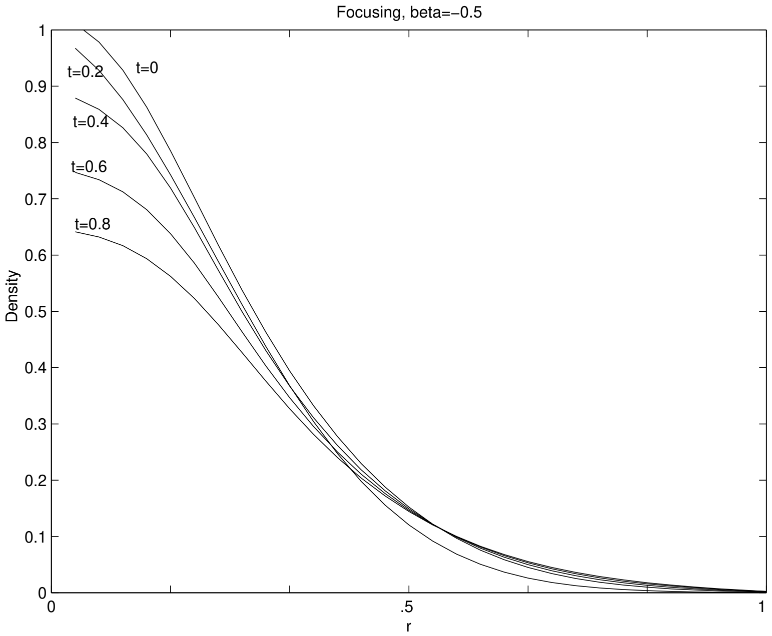


FIG. 13. *The energy density $\rho(t,r)$ in the diffusion approximation in the focusing case with $\beta=-0.5$, plotted as a function of $r$ with $\Delta t = 0.0001$. Now the condition (91) holds everywhere so there is no instability.*

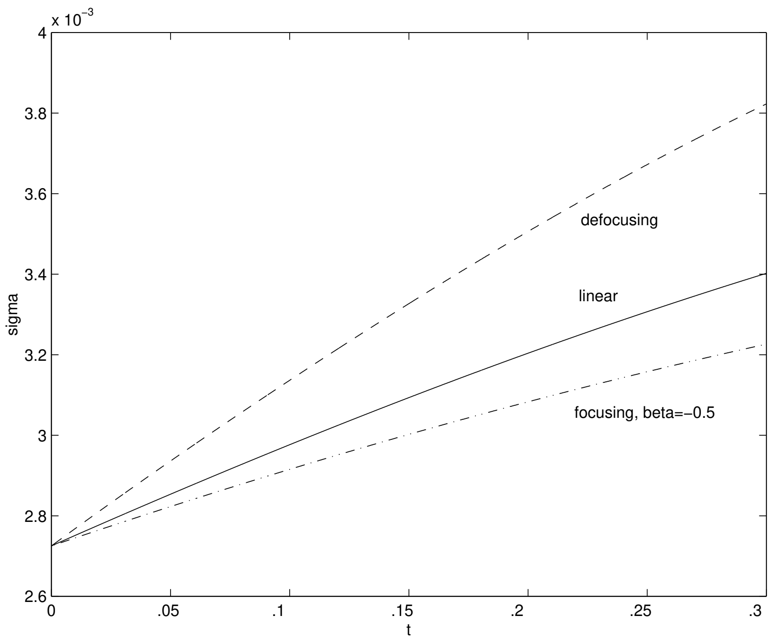


FIG. 14. *A comparison of the diffusivity $\sigma(t)$ defined in (119) for the linear, defocusing and focusing cases.*

We then use suitable numerical schemes for both the mean-field transport equation and its nonlinear diffusion approximation, and obtain numerical solutions for these two equations. Our results indicate that in the high frequency regime the random inhomogeneities prevent the wave energy from propagating in the linear and defocusing cases, but they are not strong enough to interact fully with the focusing nonlinearity. However, in the diffusive regime, randomness and nonlinearity interact fully, in a diffusive way, in all cases, defocusing and focusing. More precisely, we find that:

1. In the high frequency regime, for the linear and defocusing Schrödinger equation, the presence of the random inhomogeneities prevents the wave energy from propagating and damps its amplitude. In the focusing case, the random inhomogeneities can stabilize the focusing nonlinearity if the nonlinearity is not too strong.
2. In the diffusive regime the defocusing nonlinearity enhances the overall diffusivity. The focusing nonlinearity is anti-diffusive. However, when the strength of the nonlinearity is within a stability threshold, given by equation (91), the random diffusivity dominates and the overall solution is diffusive. Thus, if the original focusing NLS does not blow-up because the right hand side of the variance identity (4) is negative, then the random inhomogeneities can stabilize it in the high frequency and diffusive regime.

**Appendix A. The mean field approximation and the correctors.**

In this appendix, we provide some evidence supporting the mean field approximation invoked in Section 5 by analyzing the behavior of the correctors $W^{(1)}, W^{(2)}, \dots$

in the multi-scale expansion (46).

In the linear case, Spohn [16] has proved local-in-time convergence of the solution of the linear Schrödinger equation to that of the linear transport equation. Erdös and Yau [3] have improved the result so that the convergence is global in time. Both results involve detailed analysis of graphs corresponding to multiple scattering.

There are no rigorous results for the nonlinear case. The fact that the corrector analysis predicts the same limiting Boltzmann equation and the dimension ($d \geq 3$) required for convergence as proved by Erdös and Yau [3] is probably not a coincidence. The extent to which the correctors tell us about the *fluctuation* around the mean field in the limit $\epsilon \to 0$ remains to be tested and needs further investigation.

The terms in the expansion (46) are determined by substituting into the Wigner equation (44) and collecting terms of same orders in $\epsilon$:

$$O(\frac{1}{\epsilon}): \qquad \mathbf{k}\cdot\nabla_{\mathbf{y}}W = 0 \tag{120}$$

$$O(\frac{1}{\sqrt{\epsilon}}): \qquad \mathbf{k}\cdot\nabla_{\mathbf{y}}W^{(1)} + \mathcal{L}_{\frac{\mathbf{x}}{\epsilon}}W = 0 \tag{121}$$

$$O(1): \qquad \frac{\partial W}{\partial t} + \mathbf{k}\cdot\nabla_{\mathbf{x}}W + \mathcal{L}_{\frac{\mathbf{x}}{\epsilon}}W^{(1)} = -\mathbf{k}\cdot\nabla_{\mathbf{y}}W^{(2)}. \tag{122}$$

Eq. (120) means that $W = W(t,\mathbf{x},\mathbf{k})$ does not depend on the fast variable $\mathbf{y}$. Eq. (121) is the corrector equation for $W^{(1)}$ which is degenerate. With a standard regularization, Eq. (121) becomes

$$\epsilon W_\epsilon^{(1)} + \mathbf{k}\cdot\nabla_{\mathbf{y}}W_\epsilon^{(1)} + \mathcal{L}_{\frac{\mathbf{x}}{\epsilon}}W = 0 \tag{123}$$

which has the solution

$$W_\epsilon^{(1)} = i\int d\mathbf{p}\hat{V}(\mathbf{p})\frac{e^{-i\mathbf{p}\cdot\mathbf{y}}}{\epsilon - i\mathbf{k}\cdot\mathbf{p}}\left[W(t,\mathbf{x},\mathbf{k}-\mathbf{p}/2) - W(t,\mathbf{x},\mathbf{k}+\mathbf{p}/2)\right]. \tag{124}$$

Substituting (124) into Eq. (122), taking expectation and passing to the limit $\epsilon \to 0$, we get the transport equation (47) for $W$. We see from Eq. (122) that the second order corrector $W^{(2)}$ satisfies the equation

$$\mathbf{k}\cdot\nabla_{\mathbf{y}}W^{(2)} + \mathcal{L}_{\frac{\mathbf{x}}{\epsilon}}W^{(1)} - \langle\mathcal{L}_{\frac{\mathbf{x}}{\epsilon}}W^{(1)}\rangle = 0,$$

which again should be regularized as in Eq. (124). Higher order correctors can be determined similarly. We focus on the first corrector $W^{(1)}$.

As pointed out in Section 4 , the initial data for the Wigner function does not converge strongly, so neither the solution $W^\epsilon$ of the Wigner equation nor the corrector $W_\epsilon^{(1)}$ is expected to converge strongly. This is, indeed, the case as stated next.

Proposition A.1. *Suppose $W(t,\mathbf{x},\mathbf{k})$ is such that the function*

$$f(\mathbf{k},\mathbf{p}) = \hat{R}(\mathbf{p})\int d\mathbf{x}\,\left[W(\mathbf{x},\mathbf{k}-\mathbf{p}/2) - W(\mathbf{x},\mathbf{k}+\mathbf{p}/2)\right]^2$$

*is continuous and its zero set does not contain the set $\{(\mathbf{k},\mathbf{p}) : \mathbf{k}\cdot\mathbf{p} = 0\}$. Then, $\epsilon\int\int\langle|W_\epsilon^{(1)}|^2\rangle\, d\mathbf{x}d\mathbf{k}$ does not vanish as $\epsilon \to 0$, in any dimension.*

*Proof.* A straightforward calculation leads to

$$\epsilon\int\int\langle|W_\epsilon^{(1)}|^2\rangle\, d\mathbf{x}d\mathbf{k}$$

$$
\begin{aligned}
&= \int d\mathbf{p}\, \hat{R}(\mathbf{p}) \int d\mathbf{k}\, \frac{\epsilon}{\epsilon^2 + (\mathbf{k}\cdot\mathbf{p})^2} \int d\mathbf{x}\, [W(\mathbf{x},\mathbf{k}-\mathbf{p}/2) - W(\mathbf{x},\mathbf{k}+\mathbf{p}/2)]^2 \\
&\geq \frac{1}{2\epsilon} \int d\mathbf{k} \int_{|\mathbf{k}\cdot\mathbf{p}|\leq\epsilon} d\mathbf{p}\, \hat{R}(\mathbf{p}) \int d\mathbf{x}\, [W(\mathbf{x},\mathbf{k}-\mathbf{p}/2) - W(\mathbf{x},\mathbf{k}+\mathbf{p}/2)]^2 \\
&\geq \frac{1}{2\epsilon} \int d\mathbf{k} \int_{|\mathbf{k}\cdot\mathbf{p}|\leq\epsilon} d\mathbf{p}\, f(\mathbf{k},\mathbf{p}) \qquad (125)
\end{aligned}
$$

As the set $\{\mathbf{k} \in R^d : |\mathbf{k}\cdot\mathbf{p}| \leq \epsilon\} \bigcap \operatorname{supp}\{f(\mathbf{k},\mathbf{p})\}$ has a measure of order $\epsilon$ for $W$ satisfying the stated assumption, the expression (125) does not vanish in the limit $\epsilon \to 0$, as we wanted to show.

We note that "generic" functions $W$ that are *not* spherically symmetric in $\mathbf{k}$ satisfy the condition stated in Proposition A.1.

However, $\sqrt{\epsilon} W_\epsilon^{(1)}$ does vanish strongly (in $\mathbf{x}$) if it is first integrated against a test function of $\mathbf{k}$, as stated in the next proposition. This provides some reason for using the mean field hypothesis in the derivation of the transport equation.

PROPOSITION A.2. *For $d \geq 3$ and any differentiable $W(\mathbf{x},\mathbf{k})$ with a compact support, we have*

$$
\lim_{\epsilon\to 0} \epsilon \int d\mathbf{x}\, \langle \left| \int d\mathbf{k}\, W_\epsilon^{(1)} \phi(\mathbf{k}) \right|^2 \rangle = 0, \quad \forall \phi(\mathbf{k}) \in C_c^\infty \qquad (126)
$$

*Proof.* After taking the expectation, the expression on the left side of (126) becomes

$$
\epsilon \int d\mathbf{p}\, \frac{\hat{R}(\mathbf{p})}{|\mathbf{p}|^2} \int d\mathbf{x} \left| \int d\mathbf{k}\, \frac{\phi(\mathbf{k})}{\epsilon - i\mathbf{k}\cdot\hat{\mathbf{p}}} [W(\mathbf{x},\mathbf{k}-\mathbf{p}/2) - W(\mathbf{x},\mathbf{k}+\mathbf{p}/2)] \right|^2 \qquad (127)
$$

where $\hat{\mathbf{p}} = \mathbf{p}/|\mathbf{p}|$. Since $\phi(\mathbf{k})[W(\mathbf{x},\mathbf{k}-\mathbf{p}/2) - W(\mathbf{x},\mathbf{k}+\mathbf{p}/2)]$ is differentiable, we have

$$
\begin{aligned}
&\lim_{\epsilon\to 0} \int d\mathbf{k}\, \frac{\phi(\mathbf{k})}{\epsilon - i\mathbf{k}\cdot\hat{\mathbf{p}}} [W(\mathbf{x},\mathbf{k}-\mathbf{p}/2) - W(\mathbf{x},\mathbf{k}+\mathbf{p}/2)] \\
&= \lim_{\epsilon\to 0} \int_{|\mathbf{k}\cdot\hat{\mathbf{p}}|>\epsilon} d\mathbf{k}\, \frac{\phi(\mathbf{k})}{-i\mathbf{k}\cdot\hat{\mathbf{p}}} [W(\mathbf{x},\mathbf{k}-\mathbf{p}/2) - W(\mathbf{x},\mathbf{k}+\mathbf{p}/2)] \\
&= i \int d\mathbf{k}_\perp(\hat{\mathbf{p}}) ⨍ d(\mathbf{k}\cdot\hat{\mathbf{p}})\, \frac{\phi(\mathbf{k})}{\mathbf{k}\cdot\hat{\mathbf{p}}} [W(\mathbf{x},\mathbf{k}-\mathbf{p}/2) - W(\mathbf{x},\mathbf{k}+\mathbf{p}/2)] \qquad (128)
\end{aligned}
$$

with $\mathbf{k}_\perp(\hat{\mathbf{p}})$ the orthogonal projection of $\mathbf{k}$ unto the plane normal to $\mathbf{p}$. Here $⨍$ stands for the Cauchy principal value integral. Since $|\mathbf{p}|^{-2}$ in (127) is an integrable singularity in three or more dimensions, the expression in (126) is $O(\epsilon)$ as $\epsilon \to 0$, as we wanted to show.

## Acknowledgment

Shi Jin thanks the Institute for Advanced Study in Princeton and the Department of Mathematics at Stanford University for their hospitality during his extended visits there.

## REFERENCES


[1] N. Ben Abdallah and P. Degond, On a hierarchy of macroscopic models for semiconductors, J. Math. Phys. **37**, 1996, 3306-3333.

[2] G.Dell'Antonio, Large time small coupling behavior of a quantum particle in a random potential, Annals of Inst. H. Poincare, section A, **39**, 1983, 339-.

[3] L. Erdös and H.T. Yau, Linear Boltzmann equation as the weak coupling limit of a random Schrödinger equation, Comm. Pure Appl. Math.**53**, 2000, 667–735.

[4] J.Froelich and T.Spencer, Absence of diffusion in the Anderson tight binding model for large disorder or low energy, Comm. Math. Phys. **88**, 1983, 151-184.

[5] P.Gérard, P.Markovich, N.Mauser and F.Poupaud, Homogenization limits and Wigner transforms, Comm.Pure Appl. Math., **50**, 1997, 323-380.

[6] R.T. Glassey, On the blowing-up of solutions to the Cauchy problem for the nonlinear Schrödinger equation, J. Math. Phys. **18**, 1977, 1794-1797.

[7] E. Grenier, Limite semi-classique de l'equation de Schrödinger non linéaire en temps petit, CRAS Paris, **320**, 1995, 691-694.

[8] T.G.Ho, L.G.Landau and A.J.Wilkins, On the weak coupling limit for a Fermi gas in a random potential, Rev. Math. Phys., **5**, 1993, 209-298.

[9] Shan Jin, C.D. Levermore and D.W. McLaughlin, The behavior of solutions of the NLS equation in the semiclassical limit, in *Singular Limits of Dispersive Waves*, Lyon, 1991, 235-255, NATO Adv. Sci. Inst Ser. B Phys., 320, Plenum, New York, 1994.

[10] Shan Jin, C.D. Levermore and D.W. McLaughlin, The Semiclassical limit of the defocusing NLS hierarchy, Comm. Pure Appl. Math., **52**, 1999, 613-654.

[11] J.B.Keller and R.Lewis, Asymptotic methods for partial differential equations: The reduced wave equation and Maxwell's equations, in Surveys in applied mathematics, eds. J.B.Keller, D.McLaughlin and G.Papanicolaou, Plenum Press, New York, 1995.

[12] R.J. LeVeque, *Numerical Methods for Conservation Laws*, Birkhäuser, Basel, 1992.

[13] P.L. Lions and T. Paul, Sur les mesures de Wigner, Revista. Mat. Iberoamericana 9, 1993, 553-618.

[14] L.Ryzhik, G.Papanicolaou and J.Keller, Transport equations for elastic and other waves in random media, Wave Motion, **24**, 1996, 327-370.

[15] P.Sheng *Introduction to wave scattering, localization, and mesoscopic phenomena*, Academic Press, San Diego, 1995.

[16] H. Spohn, Derivation of the transport equation for electrons moving through random impurities, J. Stat. Phys., **17**, 1977, 385-412.

[17] C. Sulem and P.-L. Sulem, *Nonlinear Schrödinger equation: self-focusing and wave collapse*, Springer, 1999.

[18] E.Wigner, On the quantum correction for thermodynamic equilibrium, Physical Rev., **40**, 1932, 749-759.

[19] V.E. Zakharov, *Handbook of Plasma Physics*, edited by M.N. Rosenbluth and R.Z. Sagdeev (Elsevier, New York 1984), Vol. 2.